

# Building 1D lattice models with $G$ -graded fusion category

Shang-Qiang Ning<sup>1,2</sup>, Bin-Bin Mao<sup>3,2</sup> and Chenjie Wang<sup>2\*</sup>

<sup>1</sup> Department of Physics, The Chinese University of Hong Kong, Shatin, New Territories, Hong Kong, China

<sup>2</sup> Department of Physics and HKU-UCAS Joint Institute for Theoretical and Computational Physics, The University of Hong Kong, Pokfulam Road, Hong Kong, China

<sup>3</sup> School of Foundational Education, University of Health and Rehabilitation Sciences, Qingdao, China

\* [cjwang@hku.hk](mailto:cjwang@hku.hk)

## Abstract

We construct a family of one-dimensional (1D) quantum lattice models based on  $G$ -graded unitary fusion category  $\mathcal{C}_G$ . This family realize an interpolation between the anyon-chain models and edge models of 2D symmetry-protected topological states, and can be thought of as edge models of 2D symmetry-enriched topological states. The models display a set of unconventional global symmetries that are characterized by the input category  $\mathcal{C}_G$ . While spontaneous symmetry breaking is also possible, our numerical evidence shows that the category symmetry constrains the models to the extent that the low-energy physics has a large likelihood to be gapless.

Copyright attribution to authors.

This work is a submission to SciPost Physics.

License information to appear upon publication.

Publication information to appear upon publication.

Received Date

Accepted Date

Published Date

1

## 2 Contents

3	<b>1 Introduction</b>	<b>2</b>
4	<b>2 Model</b>	<b>4</b>
5	2.1 Basics of $G$ -graded fusion category	4
6	2.2 Hilbert space	6
7	2.3 Category symmetry	6
8	2.4 Hamiltonian	7
9	<b>3 Examples</b>	<b>8</b>
10	3.1 Anyon chain	8
11	3.2 Edge model of bosonic SPTs	9
12	3.2.1 $G = \mathbb{Z}_2$	10
13	3.3 Ising fusion category	12
14	3.4 Tambara-Yamagami category	14
15	3.5 Numerical results	15
16	3.5.1 $\kappa = 1$	16
17	3.5.2 $\kappa = -1$	16
18	3.6 $SU(2)_k$ theory	17

19	3.7 $\mathcal{C}_G$ from groups	18
20	<b>4 Discussions</b>	<b>20</b>
21	4.1 Gauge choice of $F$ and 1D SPT states	20
22	4.2 Relation to boundary of 2+1D topological phases	22
23	<b>5 Summary and outlook</b>	<b>26</b>
24	<b>A Symmetry and Hamiltonian</b>	<b>27</b>
25	A.1 Derivation of Eq. (6)	28
26	A.2 Hamiltonian is symmetric under $U(\mathbf{y}_h)$	29
27	<b>B Proof of <math>\text{Tr}(B_p) = 1</math> in <math>\mathcal{H}_{\{a_i, a_i, x_i\}}</math></b>	<b>30</b>
28	<b>References</b>	<b>31</b>
29		
30		

## 31 1 Introduction

32 It is hard to overstate the importance of symmetry in physics. Over the past decade, the role  
 33 of symmetry has been extensively studied in topological states of matter, such as symmetry-  
 34 protected topological (SPT) phases [1–3] and symmetry-enriched topological (SET) phases  
 35 [4]. A lot of novel quantum states and phenomena are discovered by studying the interplay  
 36 between symmetry and topology in quantum many-body systems.

37 The study of topological phases of matter in turn has advanced our understanding of sym-  
 38 metry. One of such advances is on ’t Hooft anomaly of symmetry [5, 6]. ’t Hooft anomaly  
 39 is invariant under renormalization group flows, so it becomes a powerful tool to constrain  
 40 the low-energy physics of a system. An anomalous system cannot admit a symmetric gapped  
 41 non-degenerate ground state, but has to break symmetry spontaneously, or be gapless, or be  
 42 topologically ordered (in two and higher dimensions) [7]. It is now understood that an anoma-  
 43 lous system can be thought of as the boundary of an SPT bulk. In fact, for a given symmetry,  
 44 ’t Hooft anomalies are in one-to-one correspondence to SPT phases in one higher dimension.  
 45 Because of the tremendous progress in the study of SPT phases in recent years, many new  
 46 types of ’t Hooft anomalies are discovered. One of the important instances is the famous Lieb-  
 47 Shultz-Mattis theorem and its generalizations [8–10], which are actually consequences of ’t  
 48 Hooft anomalies involving lattice translation [11].

49 Recently people are interested in generalizing the concept of symmetry itself. Ordinary  
 50 symmetries in quantum many-body systems are characterized by operators that act on the  
 51 whole spatial manifold and form a group mathematically. One kind of generalized symmetries  
 52 are  $\mathbf{p}$ -form symmetries, which act on submanifolds of spatial co-dimension  $\mathbf{p}$  [12, 13]. For  
 53 example, string operators associated with moving Abelian anyons in the 2D toric-code model  
 54 are 1-form symmetries [14]. Another kind of generalized symmetries are non-invertible sym-  
 55 metries, whose corresponding operators form an algebra that does not admit a definition of  
 56 inverse (i.e., beyond group). Non-invertible symmetries of a 1D system are naturally described  
 57 by a fusion category [15–19]. In high dimensions, invertible and/or non-invertible symmetries  
 58 of various co-dimensions collectively are characterized by higher fusion category, which itself  
 59 is a subject still under development [20–26]. In this work, we will refer to all these generalized  
 60 symmetries as *category symmetries*.

61 In fact, 't Hooft anomalies of ordinary finite symmetries can be well described within the  
 62 language of category. For example, consider a 1D quantum system with a finite unitary sym-  
 63 metry group  $\mathbf{G}$ . The 't Hooft anomalies are described by a 3-cocycle  $\nu_3 : \mathbf{G} \times \mathbf{G} \times \mathbf{G} \rightarrow U(1)$  [2].  
 64 The doublet  $(\mathbf{G}, \nu_3)$  forms a special fusion category, in which all simple objects are invertible.  
 65 With this connection in mind, it is then not hard to understand that general category symme-  
 66 tries are also invariant under renormalization group flow and provide strong constraints on the  
 67 low-energy physics of a theory [27]. Similar to conventional group-like symmetries, it is also  
 68 possible to define anomaly-free and anomalous category symmetries [19, 27]. In most of our  
 69 discussions and statements, we implicitly assume that the category symmetries are anomalous,  
 70 which are our main interests.

71 In this work, we pursue the idea of constraining low-energy physics with category symme-  
 72 try in the particular context of building 1D quantum lattice models. A previous example of  
 73 such lattice models is the Fibonacci anyon-chain model [28–30]. It describes a 1D array of in-  
 74 teracting Fibonacci anyons, and has a generalized symmetry described by the Fibonacci fusion  
 75 category. It turns out that the model is pinned at the tri-critical Ising conformal field theory  
 76 (CFT) at low energy by the Fibonacci category symmetry. Classical counterparts of anyon-  
 77 chain models are studied in Refs. [31, 32] and a recent on duality of category symmetry and  
 78 extension to module category is given in Ref. [33] using the framework of the tensor-network  
 79 states. Another family of such 1D lattice models are the effective edge theory of 2D SPT lattice  
 80 models, e.g., those in Refs. [34–37]. These models respect a non-onsite symmetry group  $\mathbf{G}$   
 81 with a nontrivial 3-cocycle  $\nu_3$ , or equivalently, a category symmetry  $\mathcal{C} = (\mathbf{G}, \nu_3)$ . It is found  
 82 that the low-energy physics of these models in a very large parameter space are gapless CFTs  
 83 (spontaneous symmetry breaking is another possibility).

84 We construct a family of 1D quantum lattice models based on a general  $\mathbf{G}$ -graded uni-  
 85 tary fusion category (UFC)  $\mathcal{C}_{\mathbf{G}}$ . A fusion category equipped with a  $\mathbf{G}$ -grading structure has a  
 86 decomposition  $\mathcal{C}_{\mathbf{G}} = \bigoplus_{\mathbf{g} \in \mathbf{G}} \mathcal{C}_{\mathbf{g}}$ , with  $\mathbf{G}$  being a finite group (see Sec. 2.1). In our model,  $\mathcal{C}_{\mathbf{G}}$   
 87 serves both as the input data and as the characterization of symmetries. We start by building a  
 88 1D lattice Hilbert space out of  $\mathcal{C}_{\mathbf{G}}$ , which in general does not have a tensor-product structure.  
 89 The language of fusion category allows us to naturally associate every object in  $\mathcal{C}_{\mathbf{G}}$  with an  
 90 operator, which we will use as symmetry operator. Then, we design a minimal Hamiltonian  
 91 that commutes with these symmetry operators. It turns out that our model unifies the anyon  
 92 chain model [28] and edge model of 2D bosonic SPTs [36]. When  $\mathbf{G}$  is trivial, it reduces to the  
 93 anyon chains; when  $\mathcal{C}_0$  is trivial (“0” denotes the identity of  $\mathbf{G}$ ), i.e.,  $\mathcal{C}_{\mathbf{G}} = (\mathbf{G}, \nu_3)$ , it reduces to  
 94 the SPT edge model (our model is slightly more general than Ref. [36] by having more param-  
 95 eters). Therefore, our model provides an interpolation between the anyon-chain model and  
 96 the SPT edge model. For general  $\mathcal{C}_{\mathbf{G}}$ , we find that our model can be thought of as a boundary  
 97 theory of 2D SET models (under an appropriate boundary condition) [38, 39].

98 We have numerically studied the low-energy physics of a few examples of our model. As  
 99 mentioned above, we are mainly interested in anomalous category symmetries. A sufficient  
 100 condition for a category to be anomalous is that it contains objects with non-integer quan-  
 101 tum dimensions [27], and most of our examples satisfy this condition. In the example of  
 102  $\mathcal{C}_{\mathbf{G}} = (\mathbb{Z}_2, \nu_3)$  with  $\nu_3$  being the nontrivial 3-cocycle, the phase diagram shows an *extended*  
 103 quantum critical region in the parameter space which are characterized by Luttinger liquids  
 104 (Fig. 3). When  $\mathcal{C}_{\mathbf{G}}$  is the Ising fusion category (Sec. 3.3), we find that the low-energy physics is  
 105 characterized by the critical Ising CFT at certain choices of parameters (this example is iden-  
 106 tical to that in Ref. [37]). For the  $\mathbb{Z}_3$  Tambara-Yamagami category (Sec. 3.4), we find the  
 107 low-energy physics is described by the critical 3-state Potts CFT. While more numerical effort  
 108 is needed for investigating the whole phase diagram of the latter examples, our current results  
 109 have already demonstrated that anomalous category symmetry  $\mathcal{C}_{\mathbf{G}}$  constrains the model to the  
 110 extent that the low-energy physics has a large likelihood to sit at quantum criticality.

111 The rest of the paper is outlined as follows. In Sec. 2, we build up the model. After  
 112 introducing some basic knowledge of  $G$ -graded UFC in Sec. 2.1, we construct the Hilbert space  
 113 in Sec. 2.2, write out explicit expressions of the symmetry operators in Sec. 2.3, and construct  
 114 a minimal symmetric Hamiltonian in Sec. 2.4. We then present a few examples of our model  
 115 in Sec. 3, including the two limiting cases ( $G$  being trivial and  $C_0$  being trivial), Ising fusion  
 116 category, Tambara-Yamagami category, etc. We also present some numerical results in Sec. 3.5.  
 117 We discuss the issue of the gauge choice of  $F$  symbol and its consequence to the model in  
 118 Sec. 4.1, and the relation of our model to the boundary of SET models in Sec. 4.2. In Sec. 5,  
 119 we make a summary and discuss a few future directions. Appendices include some technical  
 120 details.

## 121 2 Model

122 In this section, we describe the model. We begin with some basics of  $G$ -graded unitary fusion  
 123 category, which describes the input data of the model. The Hilbert space is constructed out of  
 124 fusion spaces of a  $G$ -graded UFC, which, in general, does not admit a tensor product structure.  
 125 Then, we write down a series of generalized symmetries and construct a general minimal  
 126 Hamiltonian that respects these symmetries. The generalized symmetries are characterized by  
 127 the input category  $C_G$  too.

### 128 2.1 Basics of $G$ -graded fusion category

129 The input data of our model is a  $G$ -graded unitary fusion category  $C_G$  [40, 41], where  $G$  is  
 130 a finite group. A category  $C_G$  contains a finite list of simple objects,<sup>1</sup> denoted as  $a, b, c$ ,  
 131 etc. Composite objects are written as a formal sum of simple objects  $\sum_a n_a a$ , with  $n_a$  a non-  
 132 negative integer. Simple objects follow a set of fusion rules  $a \times b = \sum_c N_c^{ab} c$ , where the  
 133 integer  $N_c^{ab} \geq 0$  is called fusion multiplicity. In general, fusion rules are not commutative,  
 134 i.e.  $a \times b \neq b \times a$ . There exists a special object  $\mathbb{1}$ , called the identity or vacuum, satisfying  
 135  $\mathbb{1} \times a = a \times \mathbb{1} = a$  for any  $a$ . Every simple object comes with a quantum dimension  $d_a$ , which  
 136 satisfies  $d_a d_b = \sum_c N_{ab}^c d_c$ .  $D = \sqrt{\sum_a d_a^2}$  is called the total quantum dimension. Every fusion  
 137 channel  $c$  in  $a \times b$  with  $N_{ab}^c \neq 0$  is associated with a vector space  $\mathbb{V}_c^{ab}$  of dimension  $N_{ab}^c$ , called  
 138 the fusion space. The basis state  $|ab; c, \mu\rangle \in \mathbb{V}_c^{ab}$  can be graphically represented as

$$|ab; c, \mu\rangle = \begin{array}{c} a \quad b \\ \diagdown \quad / \\ \mu \\ \diagup \quad \diagdown \\ c \end{array} . \quad (1)$$

139 An important quantity of  $C_G$  is the  $F$  symbol, which is an isomorphism  $F_d^{abc} : \bigoplus_e \mathbb{V}_e^{ab} \otimes \mathbb{V}_d^{ec} \rightarrow \bigoplus_f \mathbb{V}_d^{af} \otimes \mathbb{V}_f^{bc}$ .  
 140 With the basis vectors, it is given by

$$\begin{array}{c} a \quad b \quad c \\ \diagdown \quad / \quad \diagup \\ \mu \quad e \\ \diagup \quad \diagdown \\ \nu \\ \diagup \quad \diagdown \\ d \end{array} = \sum_{f \alpha \beta} (F_d^{abc})_{e \mu \nu}^{f \alpha \beta} \begin{array}{c} a \quad b \quad c \\ \diagdown \quad / \quad \diagup \\ f \quad \alpha \\ \diagup \quad \diagdown \\ \beta \\ \diagup \quad \diagdown \\ d \end{array} \quad (2)$$

141 Since we can perform basis transforms in  $\mathbb{V}_c^{bc}$ , the  $F$  symbols depend choices of basis. In  
 142 addition, they also satisfy consistency conditions, known as the pentagon equations [40].

<sup>1</sup>If a fusion category is braided, simple objects correspond to anyons in two-dimensional topological order. In our model, a braiding structure in  $C_G$  is not required.

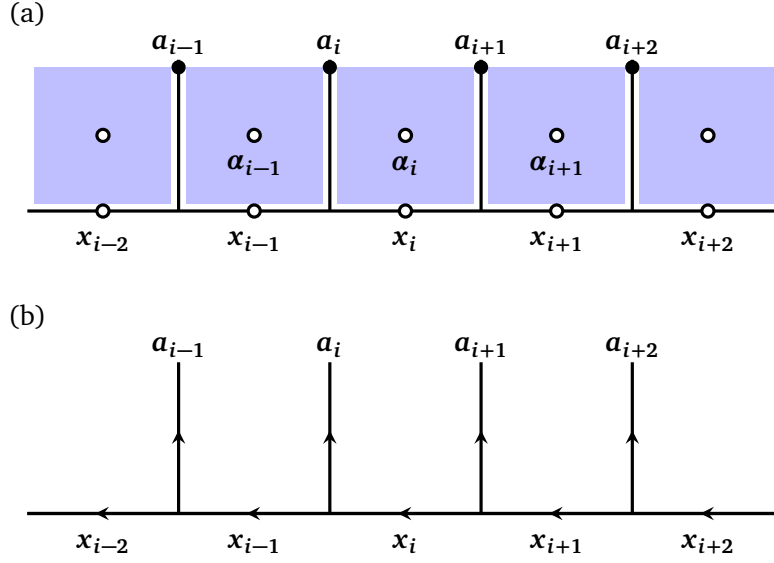


Figure 1: (a) Lattice of our 1D model. Blue regions are viewed as domains, and lines are viewed as domain walls. Each unit cell contains two dynamical variables  $\mathbf{a}_i$  and  $\mathbf{x}_i$  (empty circle), and a slaved variable  $\mathbf{a}_i$  (black dot). The “domain” variable  $\mathbf{a}_i$  is an element of a finite group  $G$ . The empty region below the horizontal line is viewed as the domain associated with the identity of  $G$ . A given configuration  $\{\mathbf{a}_i\}$  fixes the “domain wall” variables  $\{\mathbf{a}_i\}$ . Each  $\mathbf{a}_i$  is a pre-selected object in  $\mathcal{C}_{\mathbf{a}_{i-1}^{-1}\mathbf{a}_i} \subset \mathcal{C}_G$ , where  $\mathcal{C}_G$  is a  $G$ -graded fusion category. The second dynamical variable  $\mathbf{x}_i \in \mathcal{C}_{\mathbf{a}_i}$  is a fusion channel of  $\mathbf{x}_{i-1} \times \mathbf{a}_i$ . Every valid configuration  $\{\mathbf{a}_i, \mathbf{x}_i\}$  gives a quantum state  $|\{\mathbf{a}_i, \mathbf{x}_i\}\rangle$ , which all together form a basis of the lattice model. (b) The domain wall lines form a fusion tree of the objects  $\{\mathbf{a}_i\}$ .

143 Throughout the paper, we assume that  $\mathcal{C}_G$  is multiplicity-free, i.e.,  $N_{ab}^c = \mathbf{0}$  or  $\mathbf{1}$ , for simplicity.  
 144 Accordingly, the index  $\mu$  in (1) is not needed.

145 The above properties are true for any unitary fusion category. The  $G$ -grading structure  
 146 means that  $\mathcal{C}_G$  has the following decomposition

$$\mathcal{C}_G = \bigoplus_{g \in G} \mathcal{C}_g \quad (3)$$

147 with  $\mathbb{1} \in \mathcal{C}_0$ .<sup>2</sup> If  $\mathbf{a} \in \mathcal{C}_g$ , we will often denote it as  $\mathbf{a}_g$ . The grading structure is respected by  
 148 fusion,  $\mathbf{a}_g \times \mathbf{b}_h = \sum_{c_{gh}} N_{ab}^c \mathbf{c}_{gh}$ . Given a set of  $F$  symbols  $F^{\mathbf{a}_g \mathbf{b}_h \mathbf{c}_k}$ , we can modify it to obtain a  
 149 new  $G$ -graded fusion category  $\tilde{\mathcal{C}}_G$  as follows

$$\tilde{F}^{\mathbf{a}_g \mathbf{b}_h \mathbf{c}_k} = F^{\mathbf{a}_g \mathbf{b}_h \mathbf{c}_k} \nu_3(\mathbf{g}, \mathbf{h}, \mathbf{k}) \quad (4)$$

150 where  $\nu_3(\mathbf{g}, \mathbf{h}, \mathbf{k})$  is a 3-cocycle of  $G$ . If we define  $D_g = \sqrt{\sum_{\mathbf{a} \in \mathcal{C}_g} d_{\mathbf{a}}^2}$ , then  $D_g = D_0$  for all  $\mathbf{g}$ .  
 151 Then,  $D = D_0 \sqrt{|G|}$ .

152 Such  $G$ -graded fusion categories naturally appear in the study of SET phases. For more  
 153 details of unitary fusion categories, readers may consult Ref. [16, 40, 41]. For our purpose  
 154 of constructing models, we will need the set of simple objects  $\{\mathbf{a}\}$ , fusion rules described by  
 155  $\{N_{ab}^c\}$ , explicit expressions of  $F$  symbols, and the  $G$ -grading structure.

<sup>2</sup>We use either  $\mathbf{0}$  or  $\mathbf{1}$  to denote the identity of  $G$  depending on the context.

## 156 2.2 Hilbert space

157 The Hilbert space  $\mathcal{H}$  of our model is defined on a 1D lattice of length  $L$ , shown in Fig. 1. It has  
158 the following structure

$$\mathcal{H} = \bigoplus_{\{\mathbf{a}_i\}} \mathcal{H}_{\{\mathbf{a}_i\}}^{\text{fusion}}, \quad (5)$$

159 where  $\mathbf{a}_i \in \mathcal{G}$  is a “domain” variable in the  $i$ th unit cell, and  $\mathcal{H}_{\{\mathbf{a}_i\}}^{\text{fusion}}$  is the fusion space of  
160 objects  $\{\mathbf{a}_i\}$  with  $\mathbf{a}_i \in \mathcal{C}_{\mathbf{g}}$ . The set  $\{\mathbf{a}_i\}$  is determined by the domain configuration  $\{\mathbf{a}_i\}$  as  
161 follows: each  $\{\mathbf{a}_i\}$  defines a series of “domain walls” labeled by  $\mathbf{g}_i = \mathbf{a}_{i-1}^{-1} \mathbf{a}_i$  (vertical lines  
162 in Fig. 1a), and an object  $\mathbf{a}_i \in \mathcal{C}_{\mathbf{g}_i}$  is then picked out and put on the  $i$ th domain wall. We  
163 pre-select a particular object  $\mathbf{a}_{\mathbf{g}} \in \mathcal{C}_{\mathbf{g}}$  for every  $\mathbf{g}$ , such that  $\mathbf{a}_i$  is determined by  $\mathbf{g}_i$  via  $\mathbf{a}_i = \mathbf{a}_{\mathbf{g}_i}$ .  
164 Let  $\mathcal{A} = \{\mathbf{a}_{\mathbf{g}} | \forall \mathbf{g} \in \mathcal{G}\}$  be the collection of selected objects. Then, the triplet  $(\mathcal{G}, \mathcal{C}_{\mathcal{G}}, \mathcal{A})$  defines  
165 the Hilbert space  $\mathcal{H}$ .

166 Let  $\{\mathbf{x}_i\}$  be the possible fusion channels of  $\{\mathbf{a}_i\}$ . The space  $\mathcal{H}_{\{\mathbf{a}_i\}}^{\text{fusion}}$  is spanned by fusion  
167 states of  $\{\mathbf{a}_i\}$ , pictorially described by Fig. 1b. To avoid ambiguity, we take  $\mathbf{x}_i \in \mathcal{C}_{\mathbf{a}_i}$ . This  
168 corresponds to the choice that the empty region below the horizontal line in Fig. 1a is viewed  
169 as the identity domain, i.e.,  $\mathbf{a}_{\text{empty}} = \mathbf{1}$ . Accordingly,  $\mathbf{x}_i$  is the domain wall between  $\mathbf{a}_{\text{empty}}$  and  
170  $\mathbf{a}_i$ . Combining domain variables  $\{\mathbf{a}_i\}$  and fusion channels  $\{\mathbf{x}_i\}$ , we denote the basis vectors  
171 of  $\mathcal{H}$  as  $|\{\mathbf{a}_i, \mathbf{x}_i\}\rangle$ . In most part of the paper, we assume periodic boundary conditions.

172 A few remarks are in order. First, in general,  $\mathcal{H}$  does not have a tensor-product structure.  
173 In the special case that  $\mathcal{C}_0 = \{\mathbf{1}\}$ ,  $\mathcal{H}_{\{\mathbf{a}_i\}}^{\text{fusion}}$  is one-dimensional. This makes  $\mathcal{H}$  a tensor-product  
174 vector space,  $\mathcal{H} = \bigotimes_i \mathbb{V}_i^{\mathcal{G}}$ , where  $\mathbb{V}_i^{\mathcal{G}} = \text{span}\{|\{\mathbf{a}_i\}\rangle | \mathbf{a}_i \in \mathcal{G}\}$ . Second, we have selected a subset  
175  $\mathcal{A} \subset \mathcal{C}_{\mathcal{G}}$  when building up the Hilbert space. Physically, we view objects in  $\mathcal{C}_{\mathbf{g}}$  as different  
176 topological defects that can live on a  $\mathbf{g}$  domain wall. Those defects in  $\mathcal{A}$  are selected *by hand*  
177 in the current construction. Alternatively, one may allow  $\mathbf{a}_i$  to vary in  $\mathcal{C}_{\mathbf{g}_i}$  and add a term in  
178 the Hamiltonian to select the particular defect  $\mathbf{a}_{\mathbf{g}} \in \mathcal{A}$  energetically (see a discussion around  
179 Eq. (68) in Sec. 4.2). However, this will make the Hilbert space larger and less friendly for  
180 numerical calculations. Third, if  $\mathcal{C}_{\mathcal{G}}$  has nontrivial fusion multiplicities, one needs to include  
181 another variable  $\mu_i = \mathbf{1}, \dots, N_{\mathbf{x}_{i-1}\mathbf{a}_i}^{\mathbf{x}_i}$  at the vertex associated with fusing  $\mathbf{x}_{i-1}$  and  $\mathbf{a}_i$  into  $\mathbf{x}_i$ .  
182 It is neglected in our construction as we always assume that  $\mathcal{C}_{\mathcal{G}}$  is multiplicity-free.

## 183 2.3 Category symmetry

184 An advantage of using the fusion category language to build up the Hilbert space is that it helps  
185 to naturally define a set of operators which will serve as symmetry operators in our model. An  
186 interesting feature is that these operators follow the fusion algebra of  $\mathcal{C}_{\mathcal{G}}$  [Eq. (7)], which in  
187 general is not group-multiplication-like. Such kind of symmetries are called different names  
188 in the literature, e.g., algebraic symmetry, categorical symmetry or non-invertible symmetry.  
189 We will simply call them *category symmetry*, as opposed to the usual group symmetry. Even if  
190 in the special case that  $\mathcal{C}_0 = \{\mathbf{1}\}$  and the fusion algebra associated with  $\mathcal{C}_{\mathcal{G}}$  reduces to group  
191 multiplication of  $\mathcal{G}$ , we will see that the symmetry group  $\mathcal{G}$  carries a ’t Hooft anomaly in general  
192 due to nontrivial  $F$  symbols. It implies that our model is not featureless in general, but has to  
193 either break symmetries or be gapless.

194 For each simple object  $\mathbf{y}_h \in \mathcal{C}_{\mathcal{G}}$ , we can write down a symmetry operator  $U(\mathbf{y}_h)$ . Under  
195 the action of  $U(\mathbf{y}_h)$ , the domain variable  $\mathbf{a}_i$  is mapped  $\mathbf{h}\mathbf{a}_i$ , simultaneously for every  $i$ . This  
196 leaves the domain wall  $\mathbf{g}_i = \mathbf{a}_{i-1}^{-1} \mathbf{a}_i$  unchanged, so does the defect  $\mathbf{a}_i$  on it. The action on the  
197 fusion channels is associated with the matrix element

$$\langle \{\mathbf{h}\mathbf{a}_i, \mathbf{x}'_i\} | U(\mathbf{y}_h) | \{\mathbf{a}_i, \mathbf{x}_i\} \rangle = \prod_{i=1}^L \left[ (F_{\mathbf{x}'_{i+1}}^{\mathbf{y}_h, \mathbf{x}_i, \mathbf{a}_{i+1}})^\dagger \right]_{\mathbf{x}_{i+1}}^{\mathbf{x}'_i}, \quad (6)$$

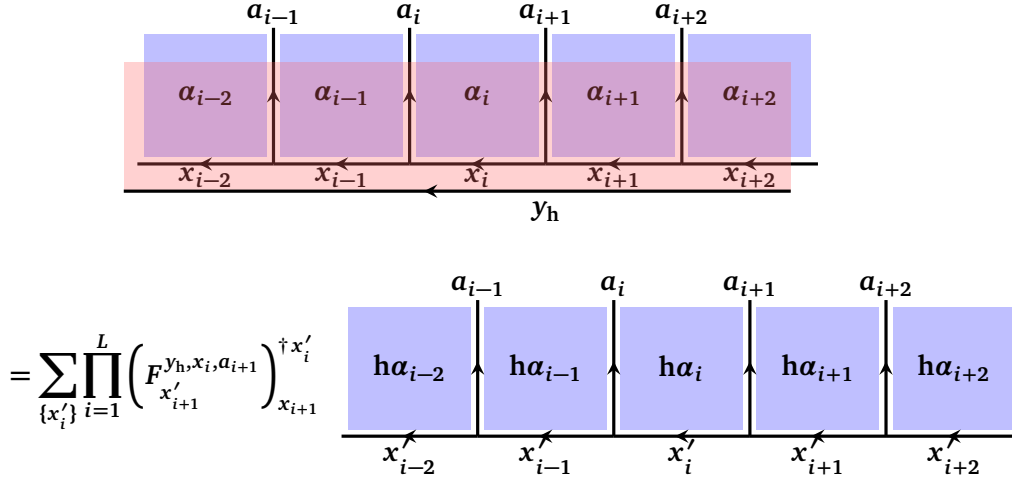


Figure 2: Graphical representation of  $U(y_h)$ . The equation is obtained by fusing a uniform  $\mathbf{h}$  domain onto  $\{\alpha_i\}$ , and a  $y_h$  line into  $\{x_i\}$ .

198 where  $x_i \in \mathcal{C}_{\alpha_i}$  and  $x'_i \in \mathcal{C}_{h\alpha_i}$ . The matrix element  $\langle \{\alpha'_i, x'_i\} | U(y_h) | \{\alpha_i, x_i\} \rangle = 0$ , if  $\alpha'_i \neq h\alpha_i$ .  
 199 The operator  $U(y_h)$  has a graphical representation, shown in Fig. 2: it is represented by fusing  
 200 a uniform  $\mathbf{h}$  domain and its  $y_h$  domain wall with respect to the vacuum into the state  $\{\alpha_i, x_i\}$ .  
 201 We show in Appendix A that the fusion process indeed gives Eq. (6).

202 The symmetry operators satisfy the algebraic relation

$$U(x_g)U(y_h) = \sum_{z_k} N_{x_g y_h}^{z_k} U(z_k) \quad (7)$$

203 This relation follows directly from that fusion processes are associative and the fusion rule is  
 204 given by  $x_g \times y_h = \sum_{z_k} N_{x_g y_h}^{z_k} z_k$ . One can also use Eq. (6) to explicitly check this algebra.  
 205 As studied in many previous works, this kind of algebraic symmetries can help (although not  
 206 guarantee) a lattice model to sit at quantum criticality. We will demonstrate this when we  
 207 discuss examples in Sec. 3.

## 208 2.4 Hamiltonian

209 With the set of symmetries  $U(y_h)$  in hand, we would like to write down a “minimal” Hamilto-  
 210 nian that respects these symmetries. We will consider a Hamiltonian of the form

$$H = - \sum_i H_i \quad (8)$$

211 and require  $H_i$  to be an operator that acts only on the  $(i-1)$ th,  $i$ th and  $(i+1)$ th unit cells.  
 212 To define  $H_i$ , it is convenient to work in an alternative basis. The alternative basis is related  
 213 to the original basis through an  $F$  move as follows:

$$\left| \begin{array}{ccc} & \alpha_i & \alpha_{i+1} \\ \alpha_{i-1} & \alpha_i & \alpha_{i+1} \\ \hline x_{i-1} & x_i & x_{i+1} \end{array} \right\rangle = \sum_{z_i} [F_{x_{i+1}}^{x_{i-1} \alpha_i \alpha_{i+1}}]_{x_i}^{z_i} \left| \begin{array}{ccc} \alpha_i & & \alpha_{i+1} \\ \alpha_{i-1} & \alpha_i & \alpha_{i+1} \\ \hline x_{i-1} & z_i & x_{i+1} \end{array} \right\rangle, \quad (9)$$



214 where  $\mathbf{z}_i$  runs over all outcomes in the fusion product  $\mathbf{a}_i \times \mathbf{a}_{i+1}$ . The term  $H_i$  in the new basis  
 215 is given by

$$\left\langle \begin{array}{c} \alpha'_i \quad \alpha'_i \quad \alpha'_{i+1} \\ \alpha'_{i-1} \quad \alpha'_{i+1} \\ \hline x'_{i-1} \quad x'_{i+1} \end{array} \middle| H_i \middle| \begin{array}{c} \alpha_i \quad \alpha_i \quad \alpha_{i+1} \\ \alpha_{i-1} \quad \alpha_{i+1} \\ \hline x_{i-1} \quad x_{i+1} \end{array} \right\rangle = w_{\alpha_i^{-1}\alpha'_i}^{z_i} \delta_{\alpha_{i-1}}^{\alpha'_{i-1}} \delta_{\alpha_{i+1}}^{\alpha'_{i+1}} \delta_{x_{i-1}}^{x'_{i-1}} \delta_{x_{i+1}}^{x'_{i+1}} \delta_{z_i}^{z'_i}, \quad (10)$$

216 where  $\delta_a^{a'} = 1$  if  $a = a'$ , and  $\delta_a^{a'} = 0$  otherwise. That is,  $H_i$  only flips the domain variable  $\mathbf{a}_i$   
 217 to  $\mathbf{a}'_i$ , with the transition amplitude denoted as  $w_{\alpha_i^{-1}\alpha'_i}^{z_i}$ . We assume the transition amplitude  
 218 only depends on the domain shift  $\mathbf{h}_i = \alpha_i^{-1}\alpha'_i$  and the fusion channel  $\mathbf{z}_i$ . One may consider  
 219 a more complicated transition amplitude. However, we find that the current choice is already  
 220 enough to produce interesting results. Hermiticity requires that  $w_{\mathbf{h}^{-1}}^{\mathbf{z}} = (w_{\mathbf{h}}^{\mathbf{z}})^*$ .

221 Using the transformation (9), the nonzero matrix elements of  $H_i$  in the original basis are  
 222 given by

$$\left\langle \begin{array}{c} \alpha'_i \quad \alpha'_{i+1} \\ \alpha_{i-1} \quad \alpha'_i \quad \alpha_{i+1} \\ \hline x_{i-1} \quad x'_i \quad x_{i+1} \end{array} \middle| H_i \middle| \begin{array}{c} \alpha_i \quad \alpha_{i+1} \\ \alpha_{i-1} \quad \alpha_i \quad \alpha_{i+1} \\ \hline x_{i-1} \quad x_i \quad x_{i+1} \end{array} \right\rangle \\ = \sum_{z_i} w_{\alpha_i^{-1}\alpha'_i}^{z_i} \left[ \left( F_{x_{i+1}}^{x_{i-1}\alpha'_i\alpha_{i+1}} \right)^\dagger \right]_{z_i}^{x'_i} \left( F_{x_{i+1}}^{x_{i-1}\alpha_i\alpha_{i+1}} \right)_{z_i}^{z_i}, \quad (11)$$

223 where the sum runs over those  $\mathbf{z}_i$ 's that are simultaneously in  $\mathbf{a}_i \times \mathbf{a}_{i+1}$  and  $\mathbf{a}'_i \times \mathbf{a}'_{i+1}$ . Note  
 224 that  $F$  symbols can be zero for certain choices of  $\mathbf{z}_i$  due to incompatible fusion. Our model is  
 225 a natural generalization of the anyon fusion chain model first proposed in Ref. [28].

226 The Hamiltonian  $H$  is symmetric under the category symmetry  $U(\mathbf{y}_h)$  in (6). An easy way  
 227 to see this is through Eq. (10). In that expression,  $H_i$  is independent of  $x_{i-1}$  and  $x_i$  and  
 228 diagonal in the variable  $\mathbf{z}_i$ . Meanwhile,  $U(\mathbf{y}_h)$  corresponds to flipping all  $\alpha_i$  and fusing a  $\mathbf{y}_g$   
 229 string, which does not change  $\mathbf{z}_i$  and only flips  $x_{i-1}$  and  $x_{i+1}$ . It is clear that the action of  $H_i$   
 230 and  $U(\mathbf{y}_h)$  commute. For a more explicit derivation, readers are referred to Appendix A.

231 We remark that  $F$  symbols depend on gauge choices. Since Eq. (11) explicitly depends  
 232 on  $F$ , our model has an explicit dependence on the gauge choice. Below we mainly focus on  
 233 examples with gauge-inequivalent  $F$  symbols. We discuss some implications of gauge choices  
 234 of  $F$  in Sec. 4.1.

### 235 3 Examples

236 The model defined in Eqs. (8) and (11) provides an ‘‘interpolation’’ of the anyon-chain model  
 237 [28] and the SPT edge model [36]. The latter two are special cases of our model. More  
 238 generally, our model can be thought of as an edge model of 2D SET phases (see Sec. 4.2).  
 239 Below we discuss how it is related to anyon chains and SPT edge models, and explore a few  
 240 other interesting examples supported by some numerical calculations.

#### 241 3.1 Anyon chain

242 When  $G$  is trivial such that  $\mathcal{C}_G = \mathcal{C}_0$ , our model reduces to the well-known anyon chain model.  
 243 In this case, there is no domain variable, i.e.,  $\alpha_i = 0$ . On domain walls, every  $\alpha_i$  is set to be a



244 simple object  $\mathbf{a} \in \mathcal{C}_0$ . The Hamiltonian (11) then reads

$$\langle x_{i-1}x'_i x_i | H_i | x_{i-1}x_i x_{i+1} \rangle = \sum_{\mathbf{z}} w^{\mathbf{z}} \left[ (F_{x_{i+1}}^{x_{i-1}aa})^\dagger \right]_{\mathbf{z}}^{x'_i} (F_{x_{i+1}}^{x_{i-1}aa})_{x_i}^{\mathbf{z}}, \quad (12)$$

245 where the site dependence of  $\mathbf{z}_i$  is dropped since all  $\mathbf{a}_i$ 's are identical. The coefficient  $w^{\mathbf{z}} \equiv w_0^{\mathbf{z}}$   
 246 is the energy of the fusion channel  $\mathbf{z}$  of two neighboring  $\mathbf{a}$ 's. This is exactly the anyon-chain  
 247 Hamiltonian that has been widely studied, e.g., in Refs. [28–30]. The simplest example is the  
 248 golden chain model, with  $\mathcal{C}_0$  being the fusion category of Fibonacci anyons. It was found the  
 249 the category symmetries  $\{U(\mathbf{y})\}$  enforce the anyon-chain model to sit at quantum criticality  
 250 [28, 42] or to break symmetry spontaneously.

### 251 3.2 Edge model of bosonic SPTs

252 Another limit of our model is  $\mathcal{C}_0 = \{\mathbb{1}\}$ . In this case,  $\mathcal{C}_G$  is equivalent to the doublet  $(G, \nu_3)$ ,  
 253 where  $\nu_3 = \nu_3(\mathbf{g}, \mathbf{h}, \mathbf{k}) \in \mathcal{H}^3(G, U(1))$  is a 3-cocycle. There is only one simple object in each  
 254  $\mathcal{C}_g$ , and the fusion algebra of  $\mathcal{C}_G$  reduces to group multiplication of  $G$ . We use the group  
 255 element  $\mathbf{g}$  to denote the simple object in  $\mathcal{C}_g$ . It has  $\mathbf{d}_g = 1$ . The  $F$  symbol is determined by  
 256  $\nu_3, (F_{ghk}^{\mathbf{g}, \mathbf{h}, \mathbf{k}})_{gh}^{\mathbf{hk}} = \nu_3(\mathbf{g}, \mathbf{h}, \mathbf{k})$ . This kind of  $G$ -graded fusion category appears in the study of  
 257 symmetry defects in 2D bosonic SPT phases with symmetry group  $G$  [2]. Below we will see  
 258 that our model can be viewed as an effective edge model for 2D bosonic SPT phases.

259 Since all simple objects in  $\mathcal{C}_G$  have quantum dimension 1, the Hilbert space has a tensor-  
 260 product structure,  $\mathcal{H} = \bigotimes_i \mathbb{V}_i^G$ , where  $\mathbb{V}_i^G = \text{span}\{|\alpha_i\rangle | \alpha_i \in G\}$ . Given a domain configura-  
 261 tion,  $\{\alpha_i\}$  and  $\{x_i\}$  are uniquely determined, with  $\mathbf{a}_i = \alpha_{i-1}^{-1} \alpha_i$  and  $x_i = \alpha_i$ . Then, our model  
 262 reduces to

$$\langle \alpha_{i-1} \alpha'_i \alpha_{i+1} | H_i | \alpha_{i-1} \alpha_i \alpha_{i+1} \rangle = w_{\mathbf{h}_i}^{\mathbf{z}_i} \frac{\nu_3(\alpha_{i-1}, \alpha_{i-1}^{-1} \alpha_i, \alpha_i^{-1} \alpha_{i+1})}{\nu_3(\alpha_{i-1}, \alpha_{i-1}^{-1} \alpha'_i, (\alpha'_i)^{-1} \alpha_{i+1})}. \quad (13)$$

263 where  $\mathbf{z}_i = \alpha_{i-1}^{-1} \alpha_{i+1}$  and  $\mathbf{h}_i = \alpha_i^{-1} \alpha'_i$ . If we take  $w_{\mathbf{h}}^{\mathbf{z}} = 1$  for every  $\mathbf{h}$  and  $\mathbf{z}$ , the model reduces  
 264 to the SPT domain-wall model of Ref. [36], which was derived by considering a domain wall of  
 265 two 2D SPT models and projecting out the bulk degrees of freedom.<sup>3</sup> It was shown numerically  
 266 there that for various choices of  $G$  and  $\nu_3$ , the low-energy spectrum is gapless and described  
 267 by a conformal field theory with an integer central charge (i.e., a Luttinger liquid). For more  
 268 general  $w_{\mathbf{h}}^{\mathbf{z}}$ , we will also give numerical evidence in Sec. 3.5 that the model is gapless and  
 269 quantum critical in an extended region of the parameter space, by considering the example  
 270  $G = \mathbb{Z}_2$  (see Fig. 3).

271 The model likes to sit at quantum criticality because it carries a 't Hooft anomaly of  $G$ . For  
 272  $\mathcal{C}_G = (G, \nu_3)$ , the symmetry operator  $U(y_g) \equiv U(\mathbf{g})$  in (6) becomes

$$\langle \mathbf{g} \alpha_1, \dots, \mathbf{g} \alpha_L | U(\mathbf{g}) | \alpha_1, \dots, \alpha_L \rangle = \prod_{i=1}^L \nu_3^*(\mathbf{g}, \alpha_i, \alpha_i^{-1} \alpha_{i+1}). \quad (14)$$

273 While the Hilbert space has a tensor-product structure, this particular realization  $\{U(\mathbf{g})\}$  of  
 274 symmetry group  $G$  is not *onsite*, making it to carry a 't Hooft anomaly. The anomaly can be  
 275 explicitly extracted through the procedure proposed in Ref. [43]. It turns out to be precisely  
 276 the 3-cocycle  $\nu_3$ . According to bulk-boundary correspondence, this model cannot be realized  
 277 on a 1D lattice, if we insist  $G$  to be realized in an onsite way. Instead, onsite realization can

<sup>3</sup>To make an exact match, the 3-cocycle  $\nu_{ab}$  in Eq. (40) of Ref. [36] is related to our 3-cocycle by  $\nu_{ab}(\alpha_1, \alpha_2, \alpha_3) = \nu_3^*(\alpha_3^{-1}, \alpha_2^{-1}, \alpha_1^{-1})$ . One also needs to convert the homogeneous cocycle in Ref. [36] to inhomogeneous cocycle and set the parameter  $\mathbf{g}^* = 1$  there.

278 only be achieved at the edge of a 2D SPT bulk characterized by the 3-cocycle  $\nu_3 \in \mathcal{H}^3(G, U(1))$   
 279 (Sec. 4.2 gives an explicit discussion of the edge viewpoint). Therefore, our 1D model mimics  
 280 the edge of a 2D bosonic SPT bulk by sacrificing the onsite-ness of the symmetry operators.  
 281 As widely known, such a 1D system cannot be featureless (i.e., gapped and symmetric with  
 282 a non-degenerate ground state). While we cannot rule out spontaneous symmetry breaking,  
 283 the 't Hooft anomaly does increase the likelihood of being gapless.

### 284 3.2.1 $G = \mathbb{Z}_2$

285 After the above general remarks, we now take a close look at the  $\mathbb{Z}_2$  case. Taking  $\mathbb{Z}_2 = \{0, 1\}$   
 286 with an additive group multiplication, we have four real parameters in the Hamiltonian (13):  
 287  $w_0^0, w_0^1, w_1^0$  and  $w_1^1$ . The cohomology group  $H^3(\mathbb{Z}_2, U(1)) = \mathbb{Z}_2$ , so there are two inequivalent  
 288 classes of  $\nu_3$ . An explicit expression of  $\nu_3$  is given by

$$\nu_3(a, b, c) = (-1)^{abc}, \quad (15)$$

289 where  $a, b, c = 0, 1$  are group elements of  $\mathbb{Z}_2$ . When  $k = 0$ ,  $\nu_3$  is trivial. When  $k = 1$ ,  $\nu_3$  is  
 290 nontrivial.

291 Let us take  $\alpha_i = \pm 1$  to represent  $\mathbb{Z}_2$  and rewrite the Hamiltonian (13) with Pauli matrices.  
 292 Let  $s_i^x, s_i^y$  and  $s_i^z$  be the Pauli matrices. It is straightforward to show that, for the trivial  $\nu_3$ ,

$$H_i^0 = \frac{w_0^0 - w_0^1}{2} s_{i-1}^z s_{i+1}^z + \frac{1}{2} [w_1^0 (1 + s_{i-1}^z s_{i+1}^z) + w_1^1 (1 - s_{i-1}^z s_{i+1}^z)] s_i^x, \quad (16)$$

293 and for the nontrivial  $\nu_3$ ,

$$H_i^1 = \frac{w_0^0 - w_0^1}{2} s_{i-1}^z s_{i+1}^z + \frac{1}{2} [w_1^0 (s_{i-1}^z + s_{i+1}^z) + w_1^1 (1 - s_{i-1}^z s_{i+1}^z)] s_i^x, \quad (17)$$

294 where a constant term  $(w_0^0 + w_0^1)/2$  has been omitted in both  $H_i^0$  and  $H_i^1$ . The symmetry  
 295 operator for the nontrivial  $\mathbb{Z}_2$  group element can be written as

$$U^0 = \prod_i s_i^x, \quad U^1 = e^{i\pi \sum_i (1 - s_i^z s_{i+1}^z)/4} \prod_i s_i^x \quad (18)$$

296 for the two models, respectively. Note that the term  $\sum_i (1 - s_i^z s_{i+1}^z)$  is always a multiple of 4  
 297 under periodic boundary condition. Also note that the two models are identical when  $w_1^0 = 0$ .  
 298 When  $w_0^0 - w_0^1 = 0$ , the model  $H^1 = -\sum_i H_i^1$  is exactly the Ising domain wall model in  
 299 Ref. [36] derived from the interface between 2D SPT bulks.

300 The model  $H^0 = -\sum_i H_i^0$  can be mapped to the usual XYZ model by the Kramers-Wannier  
 301 duality:  $s_{i-1}^z s_i^z = \mu_i^x$  and  $s_i^x = \mu_i^z \mu_{i+1}^z$ . With the mapping, we have

$$H^0 = -\sum_i (J_x \mu_i^x \mu_{i+1}^x + J_y \mu_i^y \mu_{i+1}^y + J_z \mu_i^z \mu_{i+1}^z)$$

$$J_x = \frac{w_0^0 - w_0^1}{2}, \quad J_y = \frac{w_1^1 - w_1^0}{2}, \quad J_z = \frac{w_1^1 + w_1^0}{2}. \quad (19)$$

302 The phase diagram of XYZ model is known. In particular, when  $w_1^0 = 0$ , we have  $J_y = J_z$  and  
 303 the model reduces to the XXZ model. The XXZ model exhibits three phases, with  $J_x/|J_z| = \pm 1$   
 304 being the transition points [44]: (1) ferromagnetic phase when  $J_x/|J_z| > 1$ , (2) Luttinger  
 305 liquid phase when  $-1 < J_x/|J_z| < 1$ , and (3) anti-ferromagnetic phase when  $J_x/|J_z| < -1$ .  
 306 At the transition point  $J_x/|J_z| = 1$ , the system is gapless with a quadratic spectrum. Soon as  
 307  $J_x/|J_z|$  smaller than 1, it becomes a Luttinger liquid with the Luttinger parameter  $K \rightarrow \infty$ . As

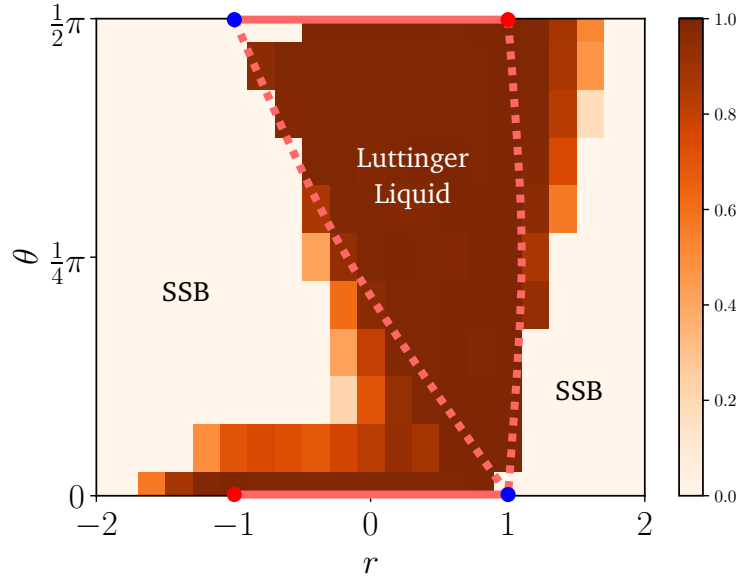


Figure 3: Color plot of central charge  $c$  extracted from entanglement entropy of the ground state of  $H^1$ , calculated by DMRG with system size up to  $L = 80$ . The dashed lines are conjectured phase boundaries which we cannot determine precisely due to finite size effects. Both the  $\theta = 0$  and  $\theta = \pi/2$  lines are equivalent to the XXZ model, but are mirror reflection of each other. The red dots are Luttinger liquids with Luttinger liquid parameter  $K = 1/2$  (equivalent to  $SU(2)_1$  CFT) and the blue dots are gapless states with quadratic dispersion. The phase diagram is symmetric under  $\theta \rightarrow -\theta$  and  $\theta \rightarrow \theta + \pi$ . “SSB” stands for spontaneous symmetry breaking.

308  $J_x/|J_z|$  decreases,  $K$  decreases until it approaches  $1/2$  at  $J_x/|J_z| = -1$ , at which the Luttinger  
 309 liquid is equivalent to  $SU(2)_1$  conformal field theory.

310 To study the phase diagram of  $H^1 = -\sum_i H_i^1$ , we first write it in a different form by per-  
 311 forming a unitary transformation. Consider the unitary operator  $S = \prod_j e^{i\pi s_j^z s_{j+1}^z / 8 + i(\pi - 2\theta) s_j^z / 4}$   
 312 and apply the transformation  $H_i^1 \rightarrow S H_i^1 S^\dagger$ , where  $\theta$  is defined via the following reparametriza-  
 313 tion,

$$J = w_0^1 - w_0^0, \quad \Delta = \sqrt{(w_1^0)^2 + (w_1^1)^2}, \quad w_1^0 = \Delta \cos \theta, \quad w_1^1 = \Delta \sin \theta \quad (20)$$

314 After the transformation, the new Hamiltonian reads

$$H_i^1 = -\frac{J}{2} s_{i-1}^z s_{i+1}^z - \frac{\Delta}{2} (\cos 2\theta s_i^x + \sin 2\theta s_i^y + s_{i-1}^z s_i^x s_{i+1}^z) \quad (21)$$

315 Accordingly, the phase diagram is symmetric under the shifting  $\theta \rightarrow \theta + \pi$ . In addition, under  
 316 the transformation  $S' = \prod_i s_i^x$ , the Hamiltonian  $H^1(\theta) \rightarrow H^1(-\theta)$ . Therefore, it is enough  
 317 to study the phase diagram for  $\theta \in [0, \pi/2]$ .

318 We have performed a density matrix renormalization group (DMRG) study of the model  
 319  $H^1 = -\sum_i H_i^1$ . We have computed the entanglement entropy of the ground state and ex-  
 320 tracted the central charge  $c$  in the  $(r, \theta)$  plane with  $r = J/\Delta$ . The results are shown in Fig. 3.  
 321 We briefly describe the phase diagram mapped out from the value of  $c$  (additional numerical  
 322 results are presented in Sec. 3.5 in comparison to other models). A key feature is that there  
 323 exists an *extended* region of gapless phase in the phase diagram. The gapless states are Lut-  
 324 tinger liquids with a varying Luttinger liquid parameter  $K$ . Also, other regions break the  $\mathbb{Z}_2$

325 symmetry spontaneously, in agreement with the expectation that no symmetric and gapped  
 326 phase is supported by an anomalous  $\mathbb{Z}_2$  symmetry. Comments on a few special lines are in  
 327 order. (1) On the  $\theta = \pi/2$  line (i.e.  $w_1^0 = 0$ ),  $H^1$  is equal to  $H^0$ , so it is equivalent to the XXZ  
 328 model. It is a Luttinger liquid when  $|r| < 1$ . (2) On the  $r$  axis ( $\theta = 0$ ),  $H^1$  is also equivalent  
 329 to the XXZ model, but it is the mirror image of the  $\theta = \pi/2$  line under  $r \rightarrow -r$ . To see that,  
 330 one may use the Kramers-Wannier duality to map (21) to the XYZ model and find that one of  
 331 the three parameters  $J_x, J_y, J_z$  differs by a minus sign compared to  $\theta = \pi/2$ . (3) For  $J = 0$   
 332 and  $\theta \in [\pi/4, \pi/2]$ , it was numerically studied in Ref. [36] that it is a Luttinger liquid, with  
 333 the Luttinger liquid parameter  $K$  varying from 1 to  $1/2$  as  $\theta$  decreases.

334 There are interesting features in the phase diagram. For example, on the phase boundary  
 335 between the Luttinger liquid and ferromagnetic (or anti-ferromagnetic) phases, the Luttinger  
 336 liquid parameter varies continuously. This indicates that the spin waves in the symmetry-  
 337 breaking phases has intriguing properties near the phase boundary. [44] In addition, it is also  
 338 interesting to study the phase diagram with other groups, e.g.,  $G = \mathbb{Z}_3$ .

### 339 3.3 Ising fusion category

340 The simplest example beyond the above two limits is that  $G = \mathbb{Z}_2$  and  $\mathcal{C}_G = \mathcal{C}_{\text{Ising}}$  the Ising  
 341 fusion category. The Ising fusion category contains three simple objects,  $\mathbb{1}, \psi$  and  $\sigma$ . The  
 342 nontrivial fusion rules are  $\sigma \times \sigma = \mathbb{1} + \psi$ ,  $\psi \times \psi = \mathbb{1}$  and  $\psi \times \sigma = \sigma$ . Quantum dimensions  
 343 are  $d_{\mathbb{1}} = d_{\psi} = 1$  and  $d_{\sigma} = \sqrt{2}$ . Let  $G = \mathbb{Z}_2 = \{0, 1\}$  with group multiplication being addition  
 344 modulo 2. The Ising category  $\mathcal{C}_{\text{Ising}}$  has the following  $\mathbb{Z}_2$  grading structure

$$C_0 = \{\mathbb{1}, \psi\}, \quad C_1 = \{\sigma\}. \quad (22)$$

345 Under certain gauge choice, the nontrivial  $F$  symbols are given by [40]

$$\begin{aligned}
 (F_{\sigma}^{\psi\sigma\psi})_{\sigma}^{\sigma} &= (F_{\psi}^{\sigma\psi\sigma})_{\sigma}^{\sigma} = -1, \\
 F_{\sigma}^{\sigma\sigma\sigma} &= \frac{\kappa}{\sqrt{2}} \begin{pmatrix} 1 & 1 \\ 1 & -1 \end{pmatrix},
 \end{aligned} \quad (23)$$

346 where  $\kappa = \pm 1$  is the Frobenius-Shur indicator distinguishing two variants of Ising fusion cat-  
 347 egory. All other  $F$  symbols are equal to 1. The two Ising fusion categories with  $\kappa = \pm 1$  can  
 348 be understood as differing by a nontrivial 3-cocycle in  $H^3(\mathbb{Z}_2, U(1)) = \mathbb{Z}_2$ . With  $\mathcal{C}_{\text{Ising}}$  as the  
 349 input, we find that our model coincides with that of Ref. [37]. This model can be properly  
 350 interpreted as the edge model of 2+1D  $\mathbb{Z}_2 \times \mathbb{Z}_2^f$  topological superconductors (fermionic SPT  
 351 phases).

352 Let us discuss some details of the model for  $\mathcal{C}_{\text{Ising}}$ . First, we pick the slaved domain-wall  
 353 variables to be  $\mathbf{a}_{g=0} = \mathbb{1}$  and  $\mathbf{a}_{g=1} = \sigma$ .<sup>4</sup> While both  $\{\mathbf{a}_i\}$  and  $\{\mathbf{x}_i\}$  are dynamical variables,  
 354 the fusion-channel variables  $\{\mathbf{x}_i\}$  are enough to uniquely label a state. Therefore, we take the  
 355 short-hand notation

$$|\mathbf{x}_{i-1}\mathbf{x}_i\mathbf{x}_{i+1}\rangle \equiv \left| \begin{array}{c|c|c} \mathbf{a}_i & \mathbf{a}_{i+1} & \\ \hline \mathbf{a}_{i-1} & \mathbf{a}_i & \mathbf{a}_{i+1} \\ \hline \mathbf{x}_{i-1} & \mathbf{x}_i & \mathbf{x}_{i+1} \end{array} \right\rangle. \quad (24)$$

<sup>4</sup>A different choice is  $\mathbf{a}_{g=0} = \psi$  and  $\mathbf{a}_{g=1} = \sigma$ .

356 With the  $F$  symbols in (23), the Hamiltonian in (11) reads

$$\begin{aligned}
H_i|\mu\mu\mu\rangle &= w_0^{\mathbb{1}}|\mu\mu\mu\rangle + w_1^{\mathbb{1}}|\mu\sigma\mu\rangle \\
H_i|\mu\mu\sigma\rangle &= w_0^{\sigma}|\mu\mu\sigma\rangle + w_1^{\sigma}|\mu\sigma\sigma\rangle \\
H_i|\mu\sigma\nu\rangle &= w_0^{\mu\times\nu}|\mu\sigma\nu\rangle + \delta_{\mu\nu}w_1^{\mathbb{1}}|\mu\mu\mu\rangle \\
H_i|\sigma\mu\mu\rangle &= w_0^{\sigma}|\sigma\mu\mu\rangle + w_1^{\sigma}|\sigma\sigma\mu\rangle \\
H_i|\mu\sigma\sigma\rangle &= w_0^{\sigma}|\mu\sigma\sigma\rangle + w_1^{\sigma}|\mu\mu\sigma\rangle \\
H_i|\sigma\mu\sigma\rangle &= \sum_{\nu} \frac{1}{2} \left[ w_0^{\mathbb{1}} + (2\delta_{\mu\nu} - 1)w_0^{\psi} \right] |\sigma\nu\sigma\rangle + \frac{\kappa w_1^{\mathbb{1}}}{\sqrt{2}} |\sigma\sigma\sigma\rangle \\
H_i|\sigma\sigma\mu\rangle &= w_0^{\sigma}|\sigma\sigma\mu\rangle + w_1^{\sigma}|\sigma\mu\mu\rangle \\
H_i|\sigma\sigma\sigma\rangle &= w_0^{\mathbb{1}}|\sigma\sigma\sigma\rangle + \frac{\kappa w_1^{\mathbb{1}}}{\sqrt{2}} (|\sigma\mathbb{1}\sigma\rangle + |\sigma\psi\sigma\rangle)
\end{aligned} \tag{25}$$

357 where  $\mu, \nu = \mathbb{1}$  or  $\psi$ . There are five real parameters in this model,  $w_0^{\mathbb{1}}, w_0^{\psi}, w_0^{\sigma}, w_1^{\mathbb{1}}$  and  
358  $w_1^{\sigma}$  (only three of them are important, while the other two set the zero energy and energy  
359 unit, respectively). When  $w_0^{\mathbb{1}} = w_0^{\psi} = w_0^{\sigma} = 0$ , our model reduces exactly to the model of  
360 Ref. [37].

361 Let us simplify the model by assuming  $w_0^{\mathbb{1}} = w_0^{\psi} \equiv w_0$ . We further perform an energy  
362 shift  $H \rightarrow H + w_0\hat{\mathbb{1}}$  and a rescaling  $H \rightarrow H/\Delta$ , with  $\Delta = \sqrt{(w_1^{\mathbb{1}})^2 + (w_1^{\sigma})^2}$ . Let

$$r = \frac{w_0^{\sigma} - w_0}{\Delta}, \quad w_1^{\mathbb{1}} = \Delta \cos \theta, \quad w_1^{\sigma} = \Delta \sin \theta \tag{26}$$

363 Then, the Hamiltonian reads

$$\begin{aligned}
H_i|\mu\mu\mu\rangle &= \cos \theta |\mu\sigma\mu\rangle \\
H_i|\mu\mu\sigma\rangle &= r|\mu\mu\sigma\rangle + \sin \theta |\mu\sigma\sigma\rangle \\
H_i|\mu\sigma\nu\rangle &= \delta_{\mu\nu} \cos \theta |\mu\mu\mu\rangle \\
H_i|\sigma\mu\mu\rangle &= r|\sigma\mu\mu\rangle + \sin \theta |\sigma\sigma\mu\rangle \\
H_i|\mu\sigma\sigma\rangle &= r|\mu\sigma\sigma\rangle + \sin \theta |\mu\mu\sigma\rangle \\
H_i|\sigma\mu\sigma\rangle &= \frac{\kappa \cos \theta}{\sqrt{2}} |\sigma\sigma\sigma\rangle \\
H_i|\sigma\sigma\mu\rangle &= r|\sigma\sigma\mu\rangle + \sin \theta |\sigma\mu\mu\rangle \\
H_i|\sigma\sigma\sigma\rangle &= \frac{\kappa \cos \theta}{\sqrt{2}} (|\sigma\mathbb{1}\sigma\rangle + |\sigma\psi\sigma\rangle)
\end{aligned} \tag{27}$$

364 There are two continuous parameters  $r$  and  $\theta$ . We will leave the complete phase diagram for  
365 future study. At the special point  $r = 0$  and  $\theta = \frac{\pi}{4}$ , we show numerically in Sec. 3.5 that the  
366 ground state is the Ising CFT, in agreement with Ref. [37].

367 Let us discuss the category symmetry in this example. The symmetry operator (6) for  
368  $\mathbf{y}_h = \sigma$  reads

$$\langle x'_1, \dots, x'_L | U(\sigma) | x_1, \dots, x_L \rangle = \prod_{i=1}^L (F_{x'_i}^{\sigma, x_i, a_{i+1}})_{x_{i+1}}^{x'_i}. \tag{28}$$

369 Since we take  $\mathbf{a}_{g=0} = \mathbb{1}$ , a valid state is always of the form

$$|\dots \sigma\sigma\mu_k\mu_k\mu_k\sigma\sigma\sigma\sigma\mu_{k+1}\mu_{k+1}\mu_{k+1}\sigma\sigma\dots\rangle \tag{29}$$

370 i.e., with segments of  $\sigma$ 's separated by segments of  $\mu$ 's. The length of each segment can vary.  
 371 Due to periodic boundary conditions, the number of  $\sigma$  segments is always equal to the number  
 372 of  $\mu$  segments. Under the action of  $U(\sigma)$ , the state in (29) will be mapped to

$$|\dots \mu'_{k-1} \mu'_{k-1} \sigma \sigma \mu'_k \mu'_k \mu'_k \mu'_k \sigma \sigma \mu'_{k+1} \mu'_{k+1} \dots\rangle \quad (30)$$

373 With the  $F$  symbols in (23), the symmetry operator (28) can be simplified to

$$\langle \{\mu'_k\} | U(\sigma) | \{\mu_k\} \rangle = \left( \frac{\kappa}{\sqrt{2}} \right)^n \prod_{k=1}^n (-1)^{(\mu_k + \mu_{k-1}) \mu'_k} \quad (31)$$

374 where  $\mu_k = \mathbf{0}, \mathbf{1}$  corresponds to  $\mathbb{1}$  and  $\psi$  respectively, and  $n$  is the number of  $\sigma$  (or  $\mu$ ) seg-  
 375 ments. Furthermore, one can explicitly check that

$$U(\sigma)^2 = U(\mathbb{1}) + U(\psi) \quad (32)$$

376 which is consistent with the fusion rule  $\sigma \times \sigma = \mathbb{1} + \psi$ . Under  $U(\psi)$ , the state  $|\{\mu_k\}\rangle$  is  
 377 mapped to  $|\{\bar{\mu}_k\}\rangle$ , with  $\bar{\mu}_k = \mathbf{1} - \mu_k$ . We note that the  $U(\sigma)$  operator is related to  $U_{11}$  in  
 378 Ref. [37] by  $U_{11} = U(\sigma)/\sqrt{2}$ . The factor  $1/\sqrt{2}$  is important to make  $U_{11}$  a *unitary* operator if  
 379 one restricts to the  $U(\psi)$  symmetric subspace (the restriction is necessary when one gauges the  
 380  $U(\psi)$  symmetry, which is indeed done in Ref. [37]). Note that  $U(\sigma)$  is not unitary, justifying  
 381 that it is a symmetry beyond the description of group.

### 382 3.4 Tambara-Yamagami category

383 Tambara-Yamagami category  $\mathcal{C}_{\text{TY}}$  is a family of  $\mathbb{Z}_2$ -graded fusion categories [45]. It is param-  
 384 eterized by a triplet  $(A, \chi, \kappa)$ , where  $A$  is an Abelian group,  $\chi$  is a symmetric non-degenerate  
 385 bicharacter  $\chi : A \times A \rightarrow U(1)$ , and  $\kappa = \pm 1$ . The simple objects of  $\mathcal{C}_{\text{TY}}$  include the elements of  
 386  $A$  and an object  $\sigma$  of quantum dimension  $\sqrt{|A|}$ , where  $|A|$  is the order of  $A$ . The  $\mathbb{Z}_2$ -grading  
 387 structure is given by

$$\mathcal{C}_0 = \{a | a \in A\}, \quad \mathcal{C}_1 = \{\sigma\} \quad (33)$$

388 Fusion rules of simple objects in  $\mathcal{C}_0$  are given by the group multiplication of  $A$ . Other fusion  
 389 rules are  $a \times \sigma = \sigma \times a = \sigma$  for any  $a \in A$ , and  $\sigma \times \sigma = \sum_{a \in A} a$ . The nontrivial  $F$  symbols  
 390 are given by

$$\begin{aligned} (F_\sigma^{a\sigma b})_\sigma^\sigma &= (F_b^{\sigma a \sigma})_\sigma^\sigma = \chi(a, b) \\ (F_\sigma^{\sigma\sigma\sigma})_a^b &= \frac{\kappa}{\sqrt{|A|}} \chi^*(a, b). \end{aligned} \quad (34)$$

391 where  $\kappa$  is the Frobenius-Shur indicator of  $\sigma$ . If we take  $A = \mathbb{Z}_N = \{\mathbb{1}, e, e^2, \dots, e^{N-1}\}$  with  
 392  $e^N = \mathbb{1}$ , the bicharacter  $\chi$  can be explicitly written as

$$\chi(e^m, e^n) = e^{\frac{i2\pi q mn}{N}}. \quad (35)$$

393 The integer  $q$  is coprime with  $N$  such that  $\chi$  is non-degenerate. For  $A = \mathbb{Z}_2$  and  $q = 1$ , we see  
 394 that  $\mathcal{C}_{\text{TY}}$  becomes  $\mathcal{C}_{\text{Ising}}$ .

395 To construct the model out of  $\mathcal{C}_{\text{TY}}$ , we take the domain wall variables to be  $\mathbf{a}_{\mathbf{g}=0} = \mathbb{1}$  and  
 396  $\mathbf{a}_{\mathbf{g}=1} = \sigma$ . Using the same short-hand notation as Eq. (24), the Hamiltonian is given by

$$\begin{aligned}
 H_i|\mu\mu\mu\rangle &= w_0^{\mathbb{1}}|\mu\mu\mu\rangle + w_1^{\mathbb{1}}|\mu\sigma\mu\rangle \\
 H_i|\mu\mu\sigma\rangle &= w_0^{\sigma}|\mu\mu\sigma\rangle + w_1^{\sigma}|\mu\sigma\sigma\rangle \\
 H_i|\mu\sigma\nu\rangle &= w_0^{\bar{\mu}\times\nu}|\mu\sigma\nu\rangle + \delta_{\mu\nu}w_1^{\mathbb{1}}|\mu\mu\mu\rangle \\
 H_i|\sigma\mu\mu\rangle &= w_0^{\sigma}|\sigma\mu\mu\rangle + w_1^{\sigma}|\sigma\sigma\mu\rangle \\
 H_i|\mu\sigma\sigma\rangle &= w_0^{\sigma}|\mu\sigma\sigma\rangle + w_1^{\sigma}|\mu\mu\sigma\rangle \\
 H_i|\sigma\mu\sigma\rangle &= \sum_{\nu, z \in A} \frac{\chi(z, \bar{\mu} \times \nu)}{|A|} w_0^z |\sigma\nu\sigma\rangle + \frac{\kappa w_1^{\mathbb{1}}}{\sqrt{|A|}} |\sigma\sigma\sigma\rangle \\
 H_i|\sigma\sigma\mu\rangle &= w_0^{\sigma}|\sigma\sigma\mu\rangle + w_1^{\sigma}|\sigma\mu\mu\rangle \\
 H_i|\sigma\sigma\sigma\rangle &= w_0^{\mathbb{1}}|\sigma\sigma\sigma\rangle + \frac{\kappa w_1^{\mathbb{1}}}{\sqrt{|A|}} \sum_{\mu \in A} |\sigma\mu\sigma\rangle
 \end{aligned} \tag{36}$$

397 where  $\mu, \nu \in A$ , and  $\bar{\mu}$  is the dual of  $\mu$  satisfying  $\mu \times \bar{\mu} = \mathbb{1}$ .

398 The bicharacter  $\chi$  appears only in the sixth line of Eq. (36). To make a simplification, we  
 399 take  $w_0^x = w_0$  for all  $x \in A$ . Then,  $\sum_{z \in A} \chi(z, \bar{\mu} \times \nu) w_0^z / |A| = \delta_{\mu, \nu} w_0$ , which simplifies the  
 400 sixth line, and the model becomes independent of  $\chi$ . In addition, we will make an energy shift  
 401  $H \rightarrow H + w_0 \mathbb{1}$  and further rescale the Hamiltonian  $H \rightarrow H/\Delta$ , with  $\Delta = \sqrt{(w_1^{\mathbb{1}})^2 + (w_1^{\sigma})^2}$ .  
 402 With the same parameterization as (26), the shifted and rescaled Hamiltonian reads

$$\begin{aligned}
 H_i|\mu\mu\mu\rangle &= \cos\theta|\mu\sigma\mu\rangle \\
 H_i|\mu\mu\sigma\rangle &= r|\mu\mu\sigma\rangle + \sin\theta|\mu\sigma\sigma\rangle \\
 H_i|\mu\sigma\nu\rangle &= \delta_{\mu\nu} \cos\theta|\mu\mu\mu\rangle \\
 H_i|\sigma\mu\mu\rangle &= r|\sigma\mu\mu\rangle + \sin\theta|\sigma\sigma\mu\rangle \\
 H_i|\mu\sigma\sigma\rangle &= r|\mu\sigma\sigma\rangle + \sin\theta|\mu\mu\sigma\rangle \\
 H_i|\sigma\mu\sigma\rangle &= \frac{\kappa \cos\theta}{\sqrt{|A|}} |\sigma\sigma\sigma\rangle \\
 H_i|\sigma\sigma\mu\rangle &= r|\sigma\sigma\mu\rangle + \sin\theta|\sigma\mu\mu\rangle \\
 H_i|\sigma\sigma\sigma\rangle &= \frac{\kappa \cos\theta}{\sqrt{|A|}} \sum_{\mu \in A} |\sigma\mu\sigma\rangle
 \end{aligned} \tag{37}$$

403 For  $A = \mathbb{Z}_2$ , it reduces to Eq. (27) of the Ising fusion category.

### 404 3.5 Numerical results

405 In this section, we present some numerical results on the models introduced in Sec. 3.2.1, 3.3  
 406 and 3.4. We compute the energy spectrum by exact diagonalization (ED) and entanglement  
 407 entropy of the ground state obtained by density matrix renormalization group (DMRG) [46].

408 We are interested in the cases that the models are gapless, which can be described by  
 409 conformal field theory (CFT). In this case, the low-lying energies of a system of finite size  $L$   
 410 take the form [47]

$$E = E_1 L + \frac{2\pi\nu}{L} \left( -\frac{c}{12} + h + \bar{h} \right), \tag{38}$$

411 where the velocity  $\nu$  is an overall scale factor and  $c$  is the central charge of the CFT. The scaling  
 412 dimensions  $h + \bar{h}$  take the form  $h = h^0 + n$ ,  $\bar{h} = \bar{h}^0 + \bar{n}$ , with  $n$  and  $\bar{n}$  non-negative integers,



413 and  $h^0$  and  $\bar{h}^0$  are the holomorphic and antiholomorphic conformal weights of the primary  
 414 fields in the given CFT. We will compare the ED spectrum to Eq. (38). Instead of using (38),  
 415 the central charge  $c$  is usually computed from the entanglement entropy  $S$  of the many-body  
 416 ground state. Under periodic boundary conditions, it is given by [48]

$$S(x) = \frac{c}{3} \ln \left( \frac{L}{\pi} \sin \left( \frac{\pi x}{L} \right) \right) + a, \quad (39)$$

417 where  $L$  is the system size,  $x$  is the length of the subsystem used to calculate the entanglement  
 418 entropy, and  $a$  is a non-universal constant. For computation of  $S(x)$ , we use DMRG to access  
 419 larger system sizes. We use the ITensor package for DMRG calculations. [49]

420 Below we present the results for the  $\mathbb{Z}_2$  SPT edge models  $H^0$  (16) and  $H^1$  (17), Ising fusion  
 421 category model (27), and Tambara-Yamagami category model (37) with  $A = \mathbb{Z}_3$ . We remark  
 422 that the Ising category model is the same as Tambara-Yamagami model with  $A = \mathbb{Z}_2$ . Also, the  
 423  $\mathbb{Z}_2$  edge models  $H^0$  and  $H^1$  are equivalent to the Tambara-Yamagami models with  $A = \mathbb{Z}_1$ , for  
 424  $\kappa = 1$  and  $\kappa = -1$  respectively. Therefore, we put the numerical results together and make  
 425 a comparison. We will leave a complete study of the phase diagrams for future study. In this  
 426 work, we mainly focus on

$$w_g^z = 1, \quad \forall z, g \quad (40)$$

427 i.e.,  $r = 0$  and  $\theta = \pi/4$  in (21), (27), and (37). These values are chosen without any priori  
 428 knowledge, but only because of simplicity. It turns out that all models with  $\kappa = 1$  are CFTs  
 429 at parameters in (40), while the cases with  $\kappa = -1$  are less conclusive. We remark that the  
 430 gapless state at the parameters (40) for the  $\kappa = 1$  Ising and  $\mathbb{Z}_3$  Tambara-Yamagami models  
 431 is *not* an isolated point in the parameter space. Our preliminary calculations show that there  
 432 exists an extended nearby gapless region, similar to Fig. 3, which we will present elsewhere  
 433 after a more careful numerical investigation.

### 434 3.5.1 $\kappa = 1$

435 Let us first consider the models with  $\kappa = 1$  and the parameters in (40). With the ground state  
 436 from DMRG calculations, we obtain the entanglement entropy  $S$  and fit the results according  
 437 to Eq. (39), as shown in Figs. 4. For the Ising and Tambara-Yamagami category models, we  
 438 find  $c \approx 1/2$  and  $c \approx 4/5$ , respectively. This indicates that, with the parameters (40), the two  
 439 models belong to the critical Ising and critical 3-state Potts universality classes, respectively.  
 440 This is verified by computing the low-energy ED spectra, which fit well with the CFT prediction  
 441 Eq. (38) (see Fig. 5).

442 The model  $H^0$  in (16) can be solved exactly by mapping to XYZ model. Nevertheless, we  
 443 did some numerical calculations for verification. It is gapped for the parameters in (40), so  
 444 instead we set  $w_0^0 - w_0^1 = 2$  and  $w_1^0 = w_1^1 = 1$  (it is equivalent to  $r = -\sqrt{2}$  and  $\theta = \pi/4$   
 445 in the Tambara-Yamagami Hamiltonian (37) with  $A = \mathbb{Z}_1$ ). With this setting, the low-energy  
 446 physics is described by double copies of the Ising CFT, see Fig. 5. It is equivalent to a free  
 447 massless complex fermion after a  $\mathbb{Z}_2$  orbifolding [50], which is a  $K = 1$  Luttinger liquid. This  
 448 agrees with the analytic results [44].

### 449 3.5.2 $\kappa = -1$

450 For  $\kappa = -1$ , all models display a much stronger finite-size effect than the case of  $\kappa = 1$ . So far,  
 451 we have only done a relatively complete search of gapless regions for the  $\mathbb{Z}_2$  edge model  $H^1$ .  
 452 The phase diagram mapped out from the central charge is shown in Fig. 3 (see discussions  
 453 in Sec. 3.2.1). In all the gapless regions, we find the central charge  $c = 1$ , i.e., a Luttinger  
 454 liquid. At the parameters  $r = 0$  and  $\theta = \pi/4$ , the numerical results of entanglement entropy

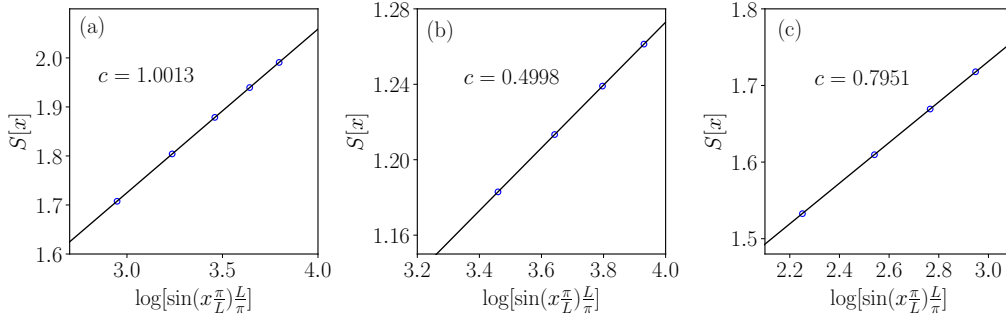


Figure 4: Entanglement entropy  $S$  of different models: (a)  $\mathbb{Z}_2$  edge model  $H^0$  with system size  $L = 60, 80, 100, 120, 140$ ; (b) Ising category model with  $L = 100, 120, 140, 160$ ; and (c) TY category model with  $L = 30, 40, 50, 60$ . All results are obtained with periodic boundary conditions and subsystem size  $x = L/2$ . For both Ising category and  $\mathbb{Z}_3$  Tambara-Yamagami category models, the parameters  $\kappa = 1$ ,  $r = 0$  and  $\theta = \pi/4$ . For the  $\mathbb{Z}_2$  edge model  $H^0$ , parameters are set at  $\omega_0^0 - \omega_0^1 = 2$  and  $\omega_1^0 = \omega_1^1 = 1$ .

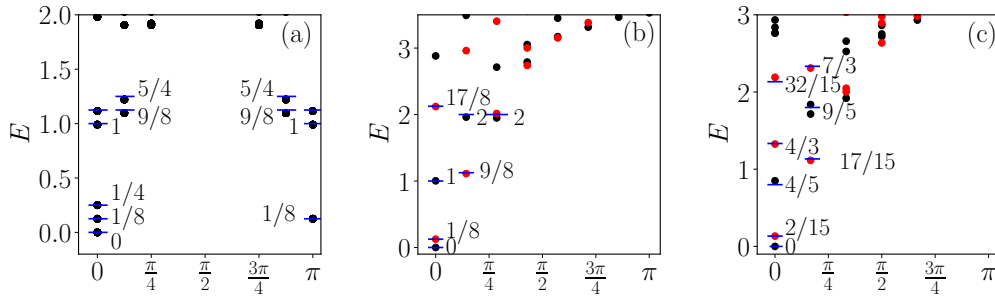


Figure 5: Finite-size energy spectra of (a)  $\mathbb{Z}_2$  edge model  $H^0$  at  $L = 16$ , (b) Ising category model  $L = 14$  and (c)  $\mathbb{Z}_3$  TY category model at  $L = 12$ , corresponding to double Ising CFT, Ising CFT and critical 3-state Potts CFT, respectively. Dots are numerical results and bars are analytic predictions [47]. Parameters are same as in Fig. 4 and energies are properly shifted and rescaled. All dots in (a) and (b) are non-degenerate. Black and red dots in (b) correspond to the eigenvalue  $+1$  and  $-1$  of  $U(\psi)$ , respectively. Every red dot in (c) is doubly degenerate, corresponding to the eigenvalue  $U(e) = e^{\pm i2\pi/3}$  respectively, with  $e$  being the generator of  $\mathbb{Z}_3$ .

455 are shown Fig. 6(a). The ED spectrum at  $L = 16$  is also shown in Fig. 6(b), but not much  
 456 information can be extracted due to strong finite size effect.

457 For Ising category and  $\mathbb{Z}_3$  Tambara-Yamagami category, we find that models are gapped at  
 458  $r = 0$  and  $\theta = \pi/4$ , as we observe  $S$  decreases to a constant as  $L$  increases (not shown here).  
 459 We have searched for gapless spectra at other values of parameters and found some evidence.  
 460 Nevertheless, it is not conclusive yet. We leave a careful numerical investigation for the future.

### 461 3.6 $SU(2)_k$ theory

462 Another family of  $\mathbb{Z}_2$ -graded category is associated with anyons from  $SU(2)_k$  theory. We de-  
 463 note the category as  $\mathcal{C}_{SU(2)_k}$ . The objects in  $\mathcal{C}_{SU(2)_k}$  are closely related to the ordinary  $SU(2)$   
 464 spins, which can be labeled by  $s = 0, \frac{1}{2}, 1, \dots, \frac{k}{2}$ , with  $k$  being a positive integer. There are

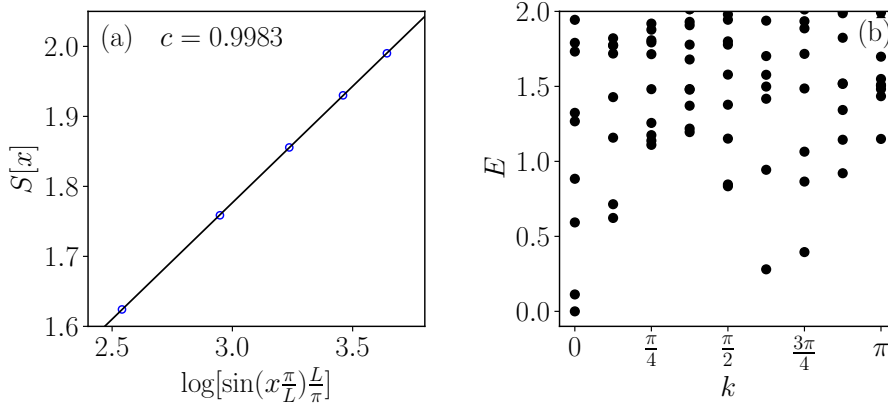


Figure 6: (a) Entanglement entropy  $S(x)$  at  $L = 40, 60, 80, 100, 120$  and (b) energy spectrum for  $H^1$  at  $L = 16$ . Parameters are  $r = 0$  and  $\theta = \pi/4$ .

465  $k + 1$  objects in total. The fusion rule between  $s$  and  $s'$  is given by

$$s \times s' = \sum_{s''=|s-s'|}^{\min(s+s', k-s-s')} s'' \quad (41)$$

466 where the summation is incremented by 1, similar to addition of ordinary angular momenta.  
 467 One can see that integer spins are closed under fusion. By taking  $\mathcal{C}_0 = \{0, 1, \dots\}$  and  $\mathcal{C}_1 = \{\frac{1}{2}, \frac{3}{2}, \dots\}$ ,  
 468 we have the following decomposition

$$\mathcal{C}_{SU(2)_k} = \mathcal{C}_0 \oplus \mathcal{C}_1. \quad (42)$$

469 This gives the  $\mathbb{Z}_2$ -grading structure of  $\mathcal{C}_{SU(2)_k}$ :  $\mathcal{C}_0$  is closed under fusion, two objects from  $\mathcal{C}_1$   
 470 fuse into objects in  $\mathcal{C}_0$ , and fusing an object from  $\mathcal{C}_0$  and an object from  $\mathcal{C}_1$  gives objects in  
 471  $\mathcal{C}_1$ . To build our model (11), we need the  $F$  symbols in  $\mathcal{C}_{SU(2)_k}$ . The  $F$  symbols are known  
 472 explicitly [51] (see also, e.g., Ref. [29]), but we will not list them here. It is interesting to  
 473 perform a detailed numerical study of this family of models in the future.

474 We give a brief further discussion on the  $k = 3$  case. It is closely related to the fa-  
 475 mous Fibonacci anyon. In this case,  $\mathcal{C}_{SU(2)_3} = \{0, 1\} \oplus \{\frac{1}{2}, \frac{3}{2}\}$ . The quantum dimensions are  
 476  $d_0 = d_{\frac{3}{2}} = 1$  and  $d_1 = d_{\frac{1}{2}} = \frac{\sqrt{5}+1}{2}$ . The object  $s = 1$  corresponds the Fibonacci anyon. There-  
 477 fore,  $\mathcal{C}_0 = \{0, 1\}$  is the usual Fibonacci category, and  $\mathcal{C}_{SU(2)_3}$  is a  $\mathbb{Z}_2$  extension of  $\mathcal{C}_0$ . (There  
 478 are two kinds of  $\mathbb{Z}_2$  extensions of the Fibonacci category, whose  $F$  symbols differ by the non-  
 479 trivial 3-cocycle in  $H^2(\mathbb{Z}_2, U(1))$ , see Eq. (4).) It is interesting to study the low-energy physics  
 480 of our model (11) based on  $\mathcal{C}_{SU(2)_3}$ , and compare it to the golden chain model [28] whose  
 481 low-energy physics is captured by the tricritical Ising conformal field theory.

### 482 3.7 $\mathcal{C}_G$ from groups

483 From group extensions, one can define many  $G$ -graded unitary fusion categories. Consider  
 484 the short exact sequence

$$1 \rightarrow N \rightarrow \mathcal{C}_G \rightarrow G \rightarrow 1 \quad (43)$$

485 where  $N$  and  $G$  are two finite groups, and  $\mathcal{C}_G$  is called an extension of  $G$  by  $N$ . The group  $N$   
 486 is a normal subgroup of  $\mathcal{C}_G$  and  $G$  is isomorphic to the quotient group  $\mathcal{C}_G/N$ . Let  $\mathcal{C}_0 \equiv N$ , and

487  $\mathcal{C}_{\mathbf{g}} \equiv \mathbf{g}N$  to be the coset in  $\mathcal{C}_G$  associated with  $\mathbf{g} \in G$ . Then,  $\mathcal{C}_G$  has the following decomposition

$$\mathcal{C}_G = \bigoplus_{\mathbf{g} \in G} \mathbf{g}N = \bigoplus_{\mathbf{g} \in G} \mathcal{C}_{\mathbf{g}} \quad (44)$$

488 Taking a 3-cocycle  $\nu_3 \in \mathcal{Z}^3(\mathcal{C}_G, U(1))$ , we can then regard the doublet  $(\mathcal{C}_G, \nu_3)$  as a  $G$ -graded  
489 fusion category. Without causing confusion, we will sometimes simply call  $\mathcal{C}_G$  the  $G$ -graded  
490 fusion category, although it is only a group in this subsection.

491 Given  $N$  and  $G$ , the extended group  $\mathcal{C}_G$  is not unique. Let  $\mathbf{a}, \mathbf{b}, \dots$  be elements of  $N$ , and  
492  $\mathbf{g}, \mathbf{h}, \dots$  be elements of  $G$ . Then, group elements in  $\mathcal{C}_G$  can be labeled by  $\mathbf{a}_{\mathbf{g}}$ , with  $\mathbf{a}$  running  
493 through elements in  $N$  and  $\mathbf{g}$  running through elements in  $G$ .<sup>5</sup> To specify the multiplication  
494 law of  $\mathcal{C}_G$ , we need two pieces of data: (i) a group homomorphism  $\rho : G \rightarrow \text{Out}(N)$ , where  
495  $\text{Out}(N)$  is the outer automorphism group of  $N$ , and (ii) a torsor  $\mu$  in  $H^2_{\rho}(G, Z(N))$ , where  $Z(N)$   
496 is the center of  $N$ . Let  $\mathbf{g} \in G$  and  $\rho_{\mathbf{g}} \equiv \rho(\mathbf{g}) \in \text{Out}(N)$ . Then,  $\rho_{\mathbf{g}}(\mathbf{a})$  describes the action of  $\mathbf{g}$   
497 on  $\mathbf{a} \in N$ . The torsor  $\mu$  is a function  $\mu : G \times G \rightarrow Z(N)$ , which satisfies the twisted 2-cocycle  
498 conditions associated with  $\rho$ . Given  $\rho$  and  $\mu$ , group multiplication in  $\mathcal{C}_G$  can be defined by

$$\mathbf{a}_{\mathbf{g}} \times \mathbf{b}_{\mathbf{h}} = [\mathbf{a} \cdot \rho_{\mathbf{g}}(\mathbf{b}) \cdot \mu(\mathbf{g}, \mathbf{h})]_{\mathbf{gh}}, \quad (45)$$

499 where “ $\cdot$ ” denotes group multiplication in  $N$ . It is clear that the group multiplication respects  
500 the  $G$ -grading structure.

501 A cocycle  $\nu_3$  in  $\mathcal{Z}^3(\mathcal{C}_G, U(1))$  can also be parameterized by a set of data associated with  $N$   
502 and  $G$ . Based on the Lyndon-Hochschild-Serre spectral sequence, it was shown in Ref. [52] that  
503  $\nu_3$  valued at general  $\mathbf{a}_{\mathbf{g}}, \mathbf{b}_{\mathbf{h}}, \mathbf{c}_{\mathbf{k}}$  can be fully determined by  $\nu_3$  at special elements of  $\mathcal{C}_G$ . Specif-  
504 ically,  $\nu_3(\mathbf{a}_{\mathbf{g}}, \mathbf{b}_{\mathbf{k}}, \mathbf{c}_{\mathbf{k}})$  is determined by  $\nu_3(\mathbf{a}, \mathbf{b}, \mathbf{c})$ ,  $\nu_3(\mathbf{a}, \mathbf{b}, \mathbf{1}_{\mathbf{g}})$ ,  $\nu_3(\mathbf{a}, \mathbf{1}_{\mathbf{g}}, \mathbf{1}_{\mathbf{h}})$  and  $\nu_3(\mathbf{1}_{\mathbf{g}}, \mathbf{1}_{\mathbf{h}}, \mathbf{1}_{\mathbf{k}})$ ,  
505 with  $\mathbf{a}, \mathbf{b}, \mathbf{c} \in N$  and  $\mathbf{g}, \mathbf{h}, \mathbf{k} \in G$  (note that  $\mathbf{a} \equiv \mathbf{a}_1$ ). We refer the readers to Ref. [52] for  
506 the general parameterization. Here, we only consider the special case that both  $\rho$  and  $\mu$  are  
507 trivial. In this case,  $\mathcal{C}_G = N \times G$ , and the 3-cocycle  $\nu_3$  is simply the product of the four special  
508 pieces

$$\nu_3(\mathbf{a}_{\mathbf{g}}, \mathbf{b}_{\mathbf{h}}, \mathbf{c}_{\mathbf{k}}) = \nu_3(\mathbf{a}, \mathbf{b}, \mathbf{c}) \nu_3(\mathbf{a}, \mathbf{b}, \mathbf{1}_{\mathbf{k}}) \nu_3(\mathbf{a}, \mathbf{1}_{\mathbf{h}}, \mathbf{1}_{\mathbf{k}}) \nu_3(\mathbf{1}_{\mathbf{g}}, \mathbf{1}_{\mathbf{h}}, \mathbf{1}_{\mathbf{k}}) \quad (46)$$

509 This expression can be well understood from the Künneth formula

$$\begin{aligned} \mathcal{H}^3(N \times G, U(1)) &= \mathcal{H}^3(N, U(1)) \oplus \mathcal{H}^1(G, \mathcal{H}^2(N, U(1))) \\ &\oplus \mathcal{H}^2(G, \mathcal{H}^2(N, U(1))) \oplus \mathcal{H}^3(G, U(1)) \end{aligned} \quad (47)$$

510 The four pieces in (46) have a one-to-one correspondence to elements in the cohomology  
511 groups on the right hand side of (47). The parameterization of  $\nu_3$  with general  $\rho$  and  $\mu$  is  
512 more complicated but follows a similar structure.

513 With  $(\mathcal{C}_G, \nu_3)$ , we can construct a lattice model following Sec. 2. For simplicity, we assume  
514 that  $\rho$  and  $\mu$  are trivial. The domain degrees of freedom  $\alpha_i$  take values in  $G$ , and domain walls  
515  $\mathbf{a}_i$  and  $\mathbf{x}_i$  take values in a proper coset  $\mathcal{C}_{\mathbf{g}} = \mathbf{g}N$ . To build up the model, we need to manually  
516 pick up a fixed element  $\bar{\mathbf{b}} \in N$  for every  $\mathbf{g} \in G$ , which together select a representative  $\bar{\mathbf{b}}_{\mathbf{g}}$  from  
517 each coset  $\mathcal{C}_{\mathbf{g}}$ . Then, on the  $i$ th domain wall, it lives an object  $\mathbf{a}_i = \bar{\mathbf{b}}_{\alpha_i^{-1} \mathbf{a}_i} \equiv (\bar{\mathbf{b}}_i)_{\alpha_i^{-1} \mathbf{a}_i}$  (we use  
518  $\bar{\mathbf{b}}_i$  to denote the  $\bar{\mathbf{b}} \in N$  that lives on the  $i$ th domain wall). The fusion channel  $\mathbf{x}_i \in \mathcal{C}_{\alpha_i}$  and let  
519 us denote  $\mathbf{x}_i \equiv (\mathbf{d}_i)_{\alpha_i}$ , with  $\mathbf{d}_i \in N$ . With fusion rules, we have  $\mathbf{x}_i = \mathbf{x}_{i-1} \mathbf{a}_i$  and  $\mathbf{d}_i = \mathbf{d}_{i-1} \bar{\mathbf{b}}_i$ .  
520 Two features of the Hilbert space deserve to be mentioned. (1) Given  $\{\alpha_i\}$  and  $\{\mathbf{a}_i\}$ , there are  
521 only  $|N|$  possible  $\{\mathbf{x}_i\}$ :

$$\mathbf{x}_i = (\mathbf{d}_i)_{\alpha_i}, \text{ with } \mathbf{d}_i = \mathbf{d}_0 \prod_{j=1}^i \bar{\mathbf{b}}_j \quad (48)$$

<sup>5</sup>This notation has a different meaning from  $\mathbf{a}_{\mathbf{g}}$  elsewhere in this paper. In this subsection,  $\mathbf{a} \in N$  and  $\mathbf{g} \in G$  are independent. In other parts of the paper,  $\mathbf{a} \in \mathcal{C}_G$  and  $\mathbf{g}$  denotes the grading property of  $\mathbf{a}$ .

522 where  $\mathbf{d}_0$  runs through elements in  $N$ . Hence, states in the Hilbert space can be labeled as  
 523  $|\{\alpha_i\}, \mathbf{d}_0\rangle$ . We will give a further discussion on  $\mathbf{d}_0$  below. (2) The periodic boundary condition  
 524 requires that

$$\prod_{i=1}^L \bar{b}_i = 1 \quad (49)$$

525 It follows from  $\mathbf{d}_{L+1} = \mathbf{d}_1 \prod_i \bar{b}_i$  and  $\mathbf{d}_{L+1} = \mathbf{d}_1$ .

526 The symmetry operator  $U(\mathbf{y}_h)$ , defined in Eq.(6), is given by

$$\begin{aligned} \langle \{\mathbf{h}\alpha_i, \mathbf{x}'_i\} | U(\mathbf{y}_h) | \{\alpha_i, \mathbf{x}_i\} \rangle &= \prod_{i=1}^L \nu_3^*(\mathbf{y}_h, (\mathbf{d}_i)_{\alpha_i}, \bar{b}_{\alpha_i^{-1}\alpha_{i+1}}), \\ &= \prod_{i=1}^L \nu_3^*(\mathbf{y}, \mathbf{d}_i, \bar{b}_i) \nu_3^*(\mathbf{y}, \mathbf{d}_i, \mathbf{1}_{\alpha_i^{-1}\alpha_{i+1}}) \\ &\quad \times \nu_3^*(\mathbf{y}, \mathbf{1}_{\alpha_i}, \mathbf{1}_{\alpha_i^{-1}\alpha_{i+1}}) \nu_3^*(\mathbf{1}_h, \mathbf{1}_{\alpha_i}, \mathbf{1}_{\alpha_i^{-1}\alpha_{i+1}}) \end{aligned} \quad (50)$$

527 where we have inserted Eq. (46) into the second equality. Note that the action of  $\mathbf{y}_h$  gives  
 528  $\mathbf{x}'_i = \mathbf{y}_h \times \mathbf{x}_i = [\mathbf{y} \cdot \mathbf{d}_i]_{\alpha'_i}$ . The Hamiltonian can be written down following Sec. 2.4.

529 Let us compare this example to that in Sec. 3.2. First, while both examples realize the sym-  
 530 metry  $(\mathcal{C}_G, \nu_3)$ , the allocation of degrees of freedom from  $N$  and  $G$  on the lattice are different.  
 531 In the example of Sec. 3.2,  $\alpha_i$  can fluctuate freely in  $\mathcal{C}_G$ . In the current example,  $\alpha_i$  fluctu-  
 532 ates only within  $G$ , while elements from  $N$  which live on the domain walls are constrained.  
 533 Accordingly, to realize the same symmetry  $(\mathcal{C}_G, \nu_3)$ , the current example could have a smaller  
 534 Hilbert space as long as one properly divides  $\mathcal{C}_G$  into  $N$  and  $G$ . This is useful for numerical  
 535 investigations. Second, the degree of freedom  $\mathbf{d}_0$ , absent in the example of Sec. 3.2, is a *global*  
 536 degree of freedom. It enters every  $\mathbf{d}_i$  and cannot be changed by any local operators. This  
 537 makes the ground states of local Hamiltonian to be  $|N|$ -fold degenerate. For simplicity, let us  
 538 consider the case  $G = \mathbf{1}$ , i.e., with no  $\{\alpha_i\}$  degrees of freedom. In this case, the whole Hilbert  
 539 space is  $|N|$  dimensional, and the Hamiltonian is proportional to the identity matrix. Since  
 540 the  $|N|$ -fold degenerate ground-state space transforms non-trivially under  $N$ , the group  $N$  is  
 541 actually “spontaneously broken”. To make the “symmetry breaking” claim more explicit, let  
 542 us allow  $\{\bar{b}_i\}$  to fluctuate (see a more general discussion around Eq. (68)). Let us denote the  
 543 states in the enlarged Hilbert space as  $|\{\mathbf{b}_i\}, \mathbf{d}_0\rangle$ , with the “-” removed to indicate that they  
 544 can fluctuate. Note that  $\{\mathbf{b}_i\}$  are subject to the constraint (49). The state  $|\{\mathbf{b}_i\}, \mathbf{d}_0\rangle$  can be  
 545 equivalently labeled as  $|\{\mathbf{d}_i\}\rangle$ , with  $\mathbf{d}_i = \mathbf{d}_{i-1}^{-1} \mathbf{b}_i$ . In the notation  $|\{\mathbf{d}_i\}\rangle$ , each  $\mathbf{d}_i$  can fluctuate  
 546 freely in  $N$ . With this preparation, the selection of  $\bar{b}_i$  corresponds to adding the action

$$H' = -\Delta \sum_i \delta_{\mathbf{d}_{i-1}^{-1} \mathbf{d}_i, \bar{b}_i} \quad (51)$$

547 and taking the limit  $\Delta \rightarrow \infty$ . The interaction  $H'$  describes a kind of “ferromagnetic” interac-  
 548 tion between  $\mathbf{d}_i$  and  $\mathbf{d}_{i-1}$ , and it is symmetric under  $N$ . In particular, if  $\bar{b}_i = \mathbf{1}$ , the interaction  
 549 becomes  $-\delta_{\mathbf{d}_{i-1}, \mathbf{d}_i}$ . It is now obvious that the ground state of  $H'$  spontaneously breaks the  
 550 symmetry group  $N$ .

## 551 4 Discussions

### 552 4.1 Gauge choice of $F$ and 1D SPT states

553 In category theory,  $F$  symbol is not a gauge invariant quantity. Given  $\mathcal{C}_G$ , one can take different  
 554 gauge choices for  $F$ . Since the Hamiltonian (11) explicitly depends the  $F$  symbol, we expect

555 the ground states to be dependent on the gauge choices of  $F$  too. In fact, gauge-equivalent  $F$   
 556 symbols can lead to *inequivalent*  $\mathcal{C}_G$ -symmetric ground states. Loosely speaking, these distinct  
 557 ground states can be thought of differing by 1D SPT states of  $\mathcal{C}_G$  category symmetry.

558 To demonstrate this point, we consider the special example  $\mathcal{C}_G = (G, \nu_3)$ , with  $\nu_3$  being a  
 559 trivial 3-cocycle. Recall from Sec. 3.2 that the  $F$  symbol is determined by  $\nu_3$ , and our model  
 560 can be thought of as an effective edge model of a 2D SPT bulk. When  $\nu_3$  is a trivial 3-cocycle,  
 561 it can be written as

$$\nu_3(\mathbf{g}, \mathbf{h}, \mathbf{k}) = \frac{c_2(\mathbf{h}, \mathbf{k})c_2(\mathbf{g}, \mathbf{hk})}{c_2(\mathbf{gh}, \mathbf{k})c_2(\mathbf{g}, \mathbf{h})} \quad (52)$$

562 where  $c_2$  is an arbitrary 2-cochain, i.e., a function  $c_2 : G \times G \rightarrow U(1)$ . Inserting (52) into the  
 563 expression (14) of  $U(\mathbf{g})$ , we have

$$U(\mathbf{g})|\alpha_1, \alpha_2, \dots, \alpha_L\rangle = \prod_i \frac{c_2(\mathbf{g}\alpha_i, \alpha_i^{-1}\alpha_{i+1})}{c_2(\alpha_i, \alpha_i^{-1}\alpha_{i+1})} |\mathbf{g}\alpha_1, \mathbf{g}\alpha_2, \dots, \mathbf{g}\alpha_L\rangle \quad (53)$$

564 If we take a local unitary transformation to the new basis

$$|\alpha_1, \dots, \alpha_L\rangle\rangle = \prod_i c_2(\alpha_i, \alpha_i^{-1}\alpha_{i+1}) |\alpha_1, \dots, \alpha_L\rangle, \quad (54)$$

565 the symmetry  $U(\mathbf{g})$  acts in the conventional onsite fashion

$$U(\mathbf{g})|\alpha_1, \alpha_2, \dots, \alpha_L\rangle\rangle = |\mathbf{g}\alpha_1, \mathbf{g}\alpha_2, \dots, \mathbf{g}\alpha_L\rangle\rangle \quad (55)$$

566 This onsite form can be achieved because  $\nu_3$  is a trivial 3-cocycle, or equivalently because the  
 567 corresponding 2D SPT bulk is trivial. In the new basis, the Hamiltonian (13) of our model is  
 568 given by

$$\langle\langle \alpha_{i-1}, \alpha'_i, \alpha_{i+1} | H_i | \alpha_{i-1}, \alpha_i, \alpha_{i+1} \rangle\rangle = w_{\mathbf{h}_i}^{z_i} \frac{c_2(\alpha_{i-1}^{-1}\alpha_i, \alpha_i^{-1}\alpha_{i+1})}{c_2(\alpha_{i-1}^{-1}\alpha'_i, \alpha_i'^{-1}\alpha_{i+1})} \quad (56)$$

569 It is straightforward to see that the Hamiltonian is symmetric under the onsite symmetry (55).

570 So far,  $c_2$  is an arbitrary 2-cochain. If we take  $w_{\mathbf{h}_i}^{z_i} = 1$  and  $c_2$  to be a 2-cocycle, i.e.,  
 571  $c_2(\mathbf{h}, \mathbf{k})c_2(\mathbf{g}, \mathbf{hk}) = c_2(\mathbf{gh}, \mathbf{k})c_2(\mathbf{g}, \mathbf{h})$ , the Hamiltonian (56) can be rewritten as

$$\langle\langle \alpha_{i-1}, \alpha'_i, \alpha_{i+1} | H_i | \alpha_{i-1}, \alpha_i, \alpha_{i+1} \rangle\rangle = \frac{c_2(\alpha_{i-1}^{-1}\alpha_i, \alpha_i^{-1}\alpha'_i)}{c_2(\alpha_i^{-1}\alpha'_i, \alpha_i'^{-1}\alpha_{i+1})} \quad (57)$$

572 It is precisely the fixed-point group-cohomology model of 1D SPT states proposed in Ref. [2].  
 573 It is known that inequivalent 2-cocycles  $c_2$  give rise to topologically distinct gapped SPT states  
 574 of symmetry group  $G$ . Therefore, we see that for the trivial  $\nu_3$ , different gauge choices (i.e.,  
 575 different  $c_2$ ) give rises to topologically distinct SPT phases. We remark that, in general,  $c_2$  is  
 576 not a 2-cocycle as we do not require our model to sit at a fixed point. Our model may also  
 577 break symmetry spontaneously.

578 If  $\nu_3$  is a non-trivial 3-cocycle, we cannot write  $\nu_3$  into the form (52). However, we can still  
 579 take different gauge choices by shifting  $\nu_3(\mathbf{g}, \mathbf{h}, \mathbf{k}) \rightarrow \nu_3(\mathbf{g}, \mathbf{h}, \mathbf{k}) \frac{c_2(\mathbf{h}, \mathbf{k})c_2(\mathbf{g}, \mathbf{hk})}{c_2(\mathbf{gh}, \mathbf{k})c_2(\mathbf{g}, \mathbf{h})}$ . A nontrivial  $\nu_3$   
 580 means the symmetry group  $G$  carries 't Hooft anomaly. The ground state cannot be simultane-  
 581 ously non-degenerate, gapped and symmetric. Let us assume a gapless and symmetric ground  
 582 state, and discuss a potential implication from different gauge choices of  $\nu_3$ . From the above  
 583 discussion on the trivial  $\nu_3$  case, we speculate that different gauge choices of non-trivial  $\nu_3$



584 correspond to the gapless state to be stacked with different 1D SPT states of the same group  $\mathbf{G}$ .  
 585 Since SPT states are gapped, stacking them will not modify the gapless spectrum dramatically.  
 586 However, topological properties of the gapless system might be modified. We do not know the  
 587 precise meaning of topological properties of a gapless system yet. It would be interesting to  
 588 explore this question in the future. We note that it might have a close relation to gapless SPT  
 589 phases discussed in Refs. [53, 54].

590 For a general category  $\mathcal{C}_G$ , it is also possible to study “generalized SPT” phases under  
 591 appropriate definitions. A reasonable definition is that an SPT state is a gapped, symmetric  
 592 and non-degenerate ground state of a Hamiltonian that respects the category symmetry  $\mathcal{C}_G$ .  
 593 However, SPT state may not always exist. For example, as just discussed, if  $\mathcal{C}_G = (\mathbf{G}, \nu_3)$   
 594 and  $\nu_3$  is a nontrivial 3-cocycle, it cannot support systems with a gapped symmetric unique  
 595 ground state. If a category symmetry does not support (trivial or nontrivial) SPT phases, it  
 596 is called *anomalous*, generalizing the concept of ’t Hooft anomaly of group-like symmetries.  
 597 Criteria on whether a category symmetry is anomalous have been studied in Ref. [27]. For  
 598 non-anomalous category symmetry, we expect that different gauge choices of  $F$  correspond  
 599 to different  $\mathcal{C}_G$ -symmetric SPT phases. For anomalous category symmetries, implications of  
 600 different gauge choices of  $F$  is subtler, as the meaning of “stacking” shall be elaborated before  
 601 we generalize the case of groups. All these are interesting questions to explore in the future.

## 602 4.2 Relation to boundary of 2+1D topological phases

603 Our model with symmetry (6) and Hamiltonian (8) can be viewed as a boundary theory of  
 604 2+1D topological phases. More precisely, in this subsection, we show that it can be viewed  
 605 as a boundary theory of 2+1D symmetry enriched string-net model (SESN) defined on a disk  
 606 geometry under certain choice of boundary conditions.

607 Let us start with a brief review of the SESN model. It is defined on a trivalent lattice with  
 608 the orientated links. The input data is a  $\mathbf{G}$ -graded unitary fusion category  $\mathcal{C}_G$ . There are two  
 609 types of degrees of freedom on the lattice. On each oriented link, there lives a  $|\mathcal{C}_G|$ -component  
 610 “spin”. Each component of the spin is a simple object  $\mathbf{a} \in \mathcal{C}_G$ , which is also called a string  
 611 type. On each plaquette, there lives a  $|\mathbf{G}|$ -component “spin”, with each component being a  
 612 group element  $\mathbf{g} \in \mathbf{G}$ , as see Fig. 7. The basis vectors of the Hilbert space can be denoted as  
 613  $\{|\mathbf{a}_l, \mathbf{g}_p\rangle\}$ , with  $l$  runs over the links and  $p$  runs over the plaquettes. The Hamiltonian is

$$H = - \sum_{\mathbf{v}} A_{\mathbf{v}} - \sum_{l} P_l - \sum_p B_p \quad (58)$$

614 where the sum runs over the vertices ( $\mathbf{v}$ ), the links ( $l$ ), and plaquettes ( $p$ ). All  $A_{\mathbf{v}}$ ,  $P_l$  and  
 615  $B_p$  are projector operators, with eigenvalues being  $\mathbf{0}$  and  $\mathbf{1}$ . The term  $A_{\mathbf{v}} = \delta_{abc}$  when acts  
 616 on basis vectors, where  $\mathbf{a}$ ,  $\mathbf{b}$  and  $\mathbf{c}$  are the three strings meeting at vertex  $\mathbf{v}$ ,  $\delta_{abc} = \mathbf{1}$  if  
 617  $\mathbf{a}, \mathbf{b}, \mathbf{c}$  satisfy the fusion rules of  $\mathcal{C}_G$  and  $\delta_{abc} = \mathbf{0}$  otherwise (again, we assume  $\mathcal{C}_G$  is fusion  
 618 multiplicity free). Assuming the string type on link  $l$  is  $\mathbf{a}_g \in \mathcal{C}_G$ , the term  $P_l = \delta_{\mathbf{g}, \mathbf{g}_p^{-1} \mathbf{g}_q}$ ,  
 619 where  $\mathbf{g}_p$  and  $\mathbf{g}_q$  are the plaquette spins on left and right of the link  $l$ , respectively (under an  
 620 appropriate orientation convention). The term  $B_p$  is defined as

$$B_p = \frac{1}{D^2} \sum_{s \in \mathcal{C}_G} d_s B_p^s \tilde{U}_p^{\mathbf{g}_s} \quad (59)$$

621 where  $d_s$  is the quantum dimension of  $s$  and  $D = \sqrt{\sum_s d_s^2}$  is the total quantum dimension.  
 622 The notation  $\mathbf{g}_s$  is used to denote  $s \in \mathcal{C}_{\mathbf{g}_s}$ . The term  $\tilde{U}_p^{\mathbf{g}_s}$  flips the plaquette spin in the following  
 623 way

$$\tilde{U}_p^{\mathbf{g}_s} |\mathbf{g}_p\rangle = |\mathbf{g}_p \mathbf{g}_s\rangle \quad (60)$$



624 where irrelevant spins are omitted in the notation  $|\mathbf{g}_p\rangle$ ). The  $\mathbf{B}_p^s$  can be understood as creating  
 625 a string  $s$  inside the plaquette  $p$  and fusing it into the boundary strings of the plaquette, so  
 626 the matrix element of  $\mathbf{B}_p^s$  is a product of  $F$  symbols. A nice property of the SESN model is that  
 627 all the projectors  $A_v$ ,  $P_l$  and  $B_p$  commute with each other, making the model exactly solvable.  
 628 The SESN model has an onsite  $G$  symmetry

$$U^g = \prod_p U_p^g, \quad U_p^g |\mathbf{g}_p\rangle = |\mathbf{g}\mathbf{g}_p\rangle \quad (61)$$

629 The SESN model realizes a topological order which mathematically is the Drinfeld center  
 630  $\mathcal{Z}(\mathcal{C}_0)$ . Since it is  $G$  symmetric, it is an SET state of the  $\mathcal{Z}(\mathcal{C}_0)$  topological order. Readers  
 631 are referred to Refs. [38, 39] for more details.

632 Now we consider the 2D SESN model on a disk geometry. In Fig. 7, the orange region  
 633 represents the string-net bulk while the blue region represents the boundary. We will see that  
 634 our 1D model lives in the subspace of the 2D SESN model after projecting the bulk into its  
 635 ground state. To match the notation of our 1D model (Fig. 1), we have labeled the corre-  
 636 sponding  $\mathbf{a}_i$ ,  $\mathbf{a}_i$ , and  $\mathbf{x}_i$  in the blue region in Fig. 7: the plaquette spins  $\mathbf{a}_i \in G$  correspond to  
 637 the domain variables in the 1D model, and the link spins  $\mathbf{a}_i \in \mathcal{C}_G$  and  $\mathbf{x}_i \in \mathcal{C}_G$  correspond to  
 638 the domain wall variables. For convenience, we will call  $\{\mathbf{a}_i, \mathbf{a}_i, \mathbf{x}_i\}$  the *boundary spins* below.  
 639 Let us consider the following Hamiltonian

$$H_{\text{disk}} = - \sum_{v \in \text{all}} A_v - \sum_{l \in \text{all}} P_l - \sum_{p \in \text{bulk}} B_p \quad (62)$$

640 where  $p$  runs only over the orange “bulk plaquette” in Fig. 7. The projectors  $A_v$ ,  $P_l$  and  $B_p$  are  
 641 the same as above. There is an ambiguity on  $P_l$  for the outermost links of the disk. To fix this  
 642 ambiguity, we assume that the empty region outside the disk is a big plaquette on which lives  
 643 a “ghost” spin  $\mathbf{g}_{\text{empty}}$ . We set the “ghost” spin  $\mathbf{g}_{\text{empty}} = \mathbf{1}$  as a choice of boundary conditions.  
 644 This choice corresponds the convention that the empty region below the horizontal line in  
 645 Fig. 1a is taken to be the identity domain. Under this convention, all  $P_l$  can be defined in the  
 646 same way. All terms in (62) commute.

647 We would like to find the ground-state subspace of  $H_{\text{disk}}$ . We will see that it is highly  
 648 degenerate, and the degeneracy comes from the states of boundary spins. First of all, we note  
 649 that, in the ground-state subspace, the requirements  $A_v = P_l = \mathbf{1}$  on the boundary spins (in  
 650 the blue region) are exactly those we impose when building up the Hilbert space of our 1D  
 651 model (Sec. 2.2). For the convenience of later discussions, we define a subspace  $\mathcal{H}_{A_v=P_l=\mathbf{1}}$  in  
 652 which  $A_v = P_l = \mathbf{1}$  are fulfilled for all  $v$ 's and  $l$ 's. The ground-state space  $\mathcal{H}_{\text{GS}} \subset \mathcal{H}_{A_v=P_l=\mathbf{1}}$ .  
 653 To find  $\mathcal{H}_{\text{GS}}$ , we note that all terms in  $H_{\text{disk}}$  does not change the boundary spins  $\{\mathbf{a}_i, \mathbf{a}_i, \mathbf{x}_i\}$ .  
 654 Then, we can diagonalize  $H_{\text{disk}}$  in the subspace with fixed  $\{\mathbf{a}_i, \mathbf{a}_i, \mathbf{x}_i\}$ . We claim that, for a  
 655 fixed set  $\{\mathbf{a}_i, \mathbf{a}_i, \mathbf{x}_i\}$  that satisfies the requirements  $A_v = P_l = \mathbf{1}$ , the ground-state subspace is  
 656 one-dimensional. That is, the ground-state subspace

$$\mathcal{H}_{\text{GS}} = \bigoplus_{\{\mathbf{a}_i, \mathbf{a}_i, \mathbf{x}_i\}} \mathcal{H}_{\{\mathbf{a}_i, \mathbf{a}_i, \mathbf{x}_i\}}^{\text{GS}} \quad (63)$$

657 where each space  $\mathcal{H}_{\{\mathbf{a}_i, \mathbf{a}_i, \mathbf{x}_i\}}^{\text{GS}}$  is one-dimensional.

658 We need to show  $\mathcal{H}_{\{\mathbf{a}_i, \mathbf{a}_i, \mathbf{x}_i\}}^{\text{GS}}$  is one-dimensional for given  $\{\mathbf{a}_i, \mathbf{a}_i, \mathbf{x}_i\}$  that satisfy  $A_v = P_l = \mathbf{1}$ .  
 659 To simplify the calculation, we make use of the fact that the SESN bulk ground state is a fixed-  
 660 point wave function, such that topological quantities, specifically ground-state degeneracy for  
 661 our purpose, are invariant if we add or remove vertices, links or plaquettes in the bulk (orange  
 662 region in Fig. 7). For detailed discussions about this property, readers may consult Ref. [55]  
 663 (strictly speaking, only the original string-net model was discussed there, but we believe it

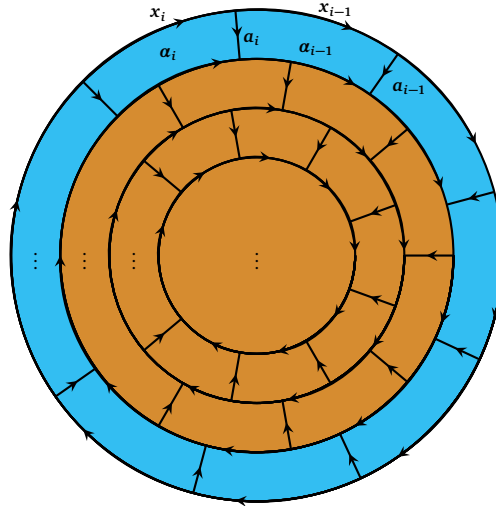


Figure 7: Trivalent lattice of 2D symmetry-enriched string-net model. The blue region corresponds to the boundary of the model.

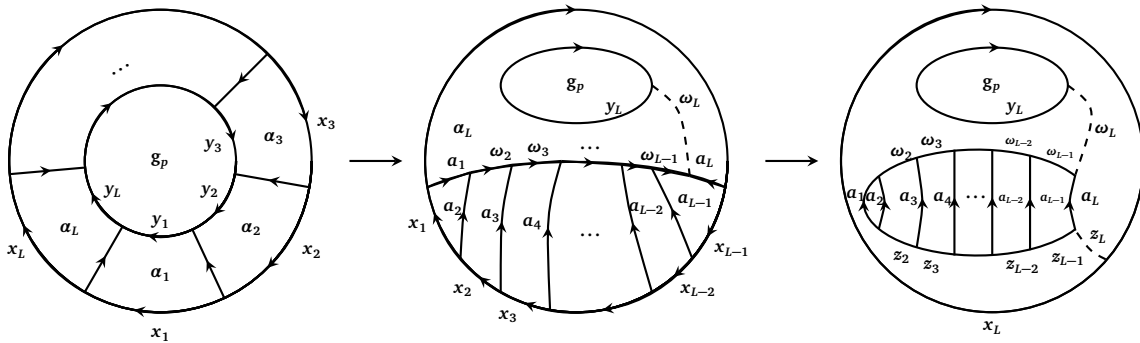


Figure 8: (a) Lattice with only one bulk plaquette. (b) and (c) States in  $\mathcal{H}_{A_v=P_l=1}$  after proper  $F$  moves. The dashed lines  $w_L$  and  $z_L$  correspond to the trivial string.

664 can be straightforwardly generalized to the SESN model). With this property, we choose a  
 665 simple graph, shown in Fig. 8(a), which contains only one bulk plaquette. On this lattice,  
 666 besides the boundary spins  $\{\mathbf{a}_i, \mathbf{a}_i, \mathbf{x}_i\}$ , the only bulk degrees of freedom are the link spins  
 667  $\{\mathbf{y}_i\}$  and a central plaquette spin  $\mathbf{g}_p$ . A general basis state is labeled as  $|\{\mathbf{a}_i, \mathbf{a}_i, \mathbf{x}_i, \mathbf{y}_i, \mathbf{g}_p\}\rangle$ . In  
 668 following discussion, we will restrict ourselves in the subspace  $\mathcal{H}_{A_v=P_l=1}$ . In this subspace, the  
 669 Hamiltonian  $\mathbf{H}_{\text{disk}}$  effectively contains only one  $\mathbf{B}_p$  term associated with the central plaquette.  
 670 To proceed, we perform “basis transformations” for  $\mathcal{H}_{A_v=P_l=1}$ . More precisely, we will  
 671 perform a transformation within the space

$$\mathcal{H}_{\{\mathbf{a}_i, \mathbf{g}_p\}} = \text{span}\{|\{\mathbf{a}_i, \mathbf{a}_i, \mathbf{x}_i, \mathbf{y}_i, \mathbf{g}_p\}\rangle | \mathbf{a}_i, \mathbf{x}_i, \mathbf{y}_i \in \mathcal{C}_G, A_v = P_l = 1, \forall v, l\}, \quad (64)$$

672 where  $\{\mathbf{a}_i\}$  and  $\mathbf{g}_p$  are fixed, and

$$\mathcal{H}_{A_v=P_l=1} = \bigoplus_{\{\mathbf{a}_i, \mathbf{g}_p\}} \mathcal{H}_{\{\mathbf{a}_i, \mathbf{g}_p\}}. \quad (65)$$

673 Because of the constraint  $A_v = 1$  for all  $v$ 's, the states in  $\mathcal{H}_{\{\mathbf{a}_i, \mathbf{g}_p\}}$  can be viewed of as fusion  
 674 states of objects  $\{\mathbf{a}_i, \mathbf{x}_i, \mathbf{y}_i\}$ . In this view, we can then perform  $\mathbf{F}$  moves which transform  
 675  $\mathcal{H}_{\{\mathbf{a}_i, \mathbf{g}_p\}}$  into a different basis. Such transformation is not a standard basis transformation on  
 676 lattice, as the underlying lattice structure is modified. However, it works well for our purpose of  
 677 counting dimensions of the constrained Hilbert space  $\mathcal{H}_{\{\mathbf{a}_i, \mathbf{g}_p\}}$ . First, we perform  $\mathbf{F}$  moves and  
 678 turn Fig. 8(a) into Fig. 8(b). Basis vectors in Fig. 8(b) are denoted as  $|\mathbf{a}_i, \mathbf{a}_i, \mathbf{x}_i, \mathbf{w}_i, \mathbf{y}_L, \mathbf{g}_p\rangle$ ,  
 679 subject to  $A_v = P_l = 1$ . An important feature is that the total fusion channel  $\mathbf{w}_L$  of  $\{\mathbf{a}_i\}$   
 680 (dashed line in Fig. 8(b)) must be 1. To see that, we recall a basic diagrammatic relation in  
 681 fusion category theory [40]:

$$\begin{array}{c} \text{c} \\ \swarrow \quad \searrow \\ \text{a} \quad \text{b} \\ \nwarrow \quad \nearrow \\ \text{c}' \end{array} = \delta_{c, c'} \begin{array}{c} | \\ \uparrow \end{array} \quad (66)$$

682 The perimeter of the central plaquette is a special case of this relation with  $c' = 1$  and  $c = \mathbf{w}_L$ .  
 683 Hence,  $\mathbf{w}_L = 1$ . Then, the  $\mathbf{y}_L$  string decouples from the rest strings.

684 Now we make two claims for states in Fig. 8(b): (i)  $\{\mathbf{w}_i\}$  are completely fixed by  $\{\mathbf{a}_i, \mathbf{a}_i, \mathbf{x}_i\}$   
 685 due to constraints  $A_v = P_l = 1$  and thereby are redundant and (ii) the remaining degeneracy  
 686 due to  $\mathbf{g}_p$  and  $\mathbf{y}_L$  is completely lifted by the  $\mathbf{B}_p$  term associated with the central plaquette in  
 687  $\mathbf{H}_{\text{disk}}$ . Under these two claims, we then immediately have  $\mathcal{H}_{\{\mathbf{a}_i, \mathbf{a}_i, \mathbf{x}_i\}}^{\text{GS}}$  is one-dimensional.

688 The first claim can be shown by performing additional  $\mathbf{F}$  moves into Fig. 8(c). Note that  
 689 these  $\mathbf{F}$  moves do not touch on  $\{\mathbf{w}_i\}$ . Accordingly, if  $\{\mathbf{w}_i\}$  are fully fixed by other spins in  
 690 Fig. 8(c), so are they in Fig. 8(b). Indeed, in the basis of Fig. 8(c), we have  $\mathbf{w}_i = \mathbf{z}_i$  for every  
 691  $i$ . This is obtained by repeatedly applying the relation (66) to Fig. 8(c).

692 Given the first claim, we then have all valid states in  $\mathcal{H}_{A_v=P_l=1}$  with fixed  $\{\mathbf{a}_i, \mathbf{a}_i, \mathbf{x}_i\}$  form  
 693 the following space

$$\mathcal{H}_{\{\mathbf{a}_i, \mathbf{a}_i, \mathbf{x}_i\}} = \text{span}\{|\mathbf{y}_L, \mathbf{g}_p\rangle | \mathbf{y}_L \in \mathcal{C}_G, \mathbf{g}_p = \mathbf{a}_L \mathbf{g}_{\mathbf{y}_L}\} \quad (67)$$

694 where the condition  $\mathbf{g}_p = \mathbf{a}_L \mathbf{g}_{\mathbf{y}_L}$  follows from the constraint  $P_l = 1$ . We note that  $\mathcal{H}_{\{\mathbf{a}_i, \mathbf{a}_i, \mathbf{x}_i\}}$   
 695 is always  $|\mathcal{C}_G|$ -dimensional. The action of  $\mathbf{H}_{\text{disk}} = -\mathbf{B}_p$  is closed in  $\mathcal{H}_{\{\mathbf{a}_i, \mathbf{a}_i, \mathbf{x}_i\}}$ . To prove the  
 696 second claim, we need to calculate the ground state degeneracy inside  $\mathcal{H}_{\{\mathbf{a}_i, \mathbf{a}_i, \mathbf{x}_i\}}$ . We recall  
 697 that  $\mathbf{B}_p$  is a projector, i.e.,  $\mathbf{B}_p^2 = \mathbf{B}_p$ . Hence, the ground states have  $\mathbf{B}_p$  eigenvalue 1 and the  
 698 excited states have  $\mathbf{B}_p$  eigenvalue 0. Then, the ground state degeneracy is given by  $\text{Tr}(\mathbf{B}_p)$ .

699 We show in Appendix B that  $\text{Tr}(\mathbf{B}_p) = 1$  in  $\mathcal{H}_{\{\mathbf{a}_i, \mathbf{a}_i, \mathbf{x}_i\}}$  for arbitrary  $\{\mathbf{a}_i, \mathbf{a}_i, \mathbf{x}_i\}$ , i.e.,  $\mathcal{H}_{\{\mathbf{a}_i, \mathbf{a}_i, \mathbf{x}_i\}}^{\text{GS}}$   
 700 is one-dimensional.

701 To summarize, we have shown that the ground-state space  $\mathcal{H}_{\text{GS}}$  of  $H_{\text{disk}}$  in (62) is of the  
 702 form (63), with  $\mathcal{H}_{\{\mathbf{a}_i, \mathbf{a}_i, \mathbf{x}_i\}}^{\text{GS}}$  being one-dimensional. That is,  $\mathcal{H}_{\text{GS}}$  is fully described by the bound-  
 703 ary spins  $\{\mathbf{a}_i, \mathbf{a}_i, \mathbf{x}_i\}$  subject to the constraints  $\mathbf{A}_v = \mathbf{P}_l = \mathbf{1}$  for all relevant vertices and links.  
 704 To exactly match our 1D model, we introduce additional interaction between the boundary  
 705 spins

$$H' = H_{\text{1D}} - \Delta \sum_{l_a} K_{l_a} \quad (68)$$

706 where  $H_{\text{1D}}$  is the 1D Hamiltonian in Sec. 2.4, and  $\Delta$  is a large positive number. The sum in the  
 707 second piece runs over all links  $l_a$  that  $\{\mathbf{a}_i\}$  lives. When acting on basis states, the operator  
 708  $K_{l_a} = \delta(\mathbf{a}_i, \bar{\mathbf{a}}_{\alpha_i^{-1} \mathbf{a}_i})$ , where  $\bar{\mathbf{a}}_g$  is the selected object from  $\mathcal{C}_g$  discussed in Sec. 2.2 (we have  
 709 added a bar in the notation to distinguish it from  $\mathbf{a}_i$  on links). In the limit  $\Delta \rightarrow \infty$ , this  
 710 boundary theory matches exactly to our 1D model.

711 In the above discussions, we have focused on the Hilbert space and Hamiltonian, and have  
 712 not touched on symmetry. The SESN model has an onsite  $\mathbf{G}$  group symmetry, while the 1D  
 713 model is *not* symmetric under onsite  $\mathbf{G}$ , instead is symmetric under  $\mathcal{C}_G$ . To understand this, let  
 714 us apply  $U^g$  of (60) onto  $\mathcal{H}_{\text{GS}}$ . Let  $|\{\mathbf{a}_i, \mathbf{a}_i, \mathbf{x}_i\}\rangle$  be the state in  $\mathcal{H}_{\{\mathbf{a}_i, \mathbf{a}_i, \mathbf{x}_i\}}^{\text{GS}}$ . Due to the constraints  
 715  $\mathbf{P}_l = \mathbf{1}$  and the boundary condition  $\mathbf{g}_{\text{empty}} = \mathbf{1}$ , we have  $\mathbf{x}_i \in \mathcal{C}_{\alpha_i}$  and  $\mathbf{a}_i \in \mathcal{C}_{\alpha_i^{-1} \mathbf{a}_i}$ . Then,  
 716  $U^g |\{\mathbf{a}_i, \mathbf{a}_i, \mathbf{x}_i\}\rangle \sim |g\mathbf{a}_i, \mathbf{a}_i, \mathbf{x}'_i\rangle$  with  $\mathbf{x}'_i \in \mathcal{C}_{g\alpha_i}$ . On the one hand, since  $\mathbf{x}'_i \notin \mathcal{C}_{\alpha_i}$ , the ground-  
 717 state  $|\{\mathbf{a}_i, \mathbf{a}_i, \mathbf{x}_i\}\rangle$  transforms nontrivially under  $\mathbf{G}$ , making it broken in some sense. On the  
 718 other hand, the choice of  $\{\mathbf{x}'_i\}$  is not unique. To fix this ambiguity, we think of  $U^g = \prod_p U_p^g$   
 719 as a union of all plaquettes and take a string  $s \in \mathcal{C}_g$  as its termination on the boundary. This  
 720 termination means that, after applying  $U^g$ , we further fuse  $s$  onto  $\{\mathbf{x}_i\}$  from outside. Let us  
 721 denote the string fusion operator as  $\mathbf{B}_0^s$ , such that the combination sends  $|\{\mathbf{a}_i, \mathbf{a}_i, \mathbf{x}_i\}\rangle$  to the  
 722 state  $\mathbf{B}_0^s U^g |\{\mathbf{a}_i, \mathbf{a}_i, \mathbf{x}_i\}\rangle$ . One may notice that it is similar to the  $\mathbf{B}_p$  operator in the Hamiltonian,  
 723 except that  $U^g$  has a left group action and  $\mathbf{B}_0^s$  fuses the  $s$  string from outside of the plaquette in  
 724 comparison to “right action” and “fusion from inside” for  $\mathbf{B}_p$  in the Hamiltonian. The collection  
 725  $\{\mathbf{B}_0^s U^g\}$  with  $s$  running over all simple objects in  $\mathcal{C}_G$  are exactly the category symmetries  
 726 discussed in Sec. 2.3.

727 Finally, we remark that while we have taken the limit  $\Delta \rightarrow \infty$  in (68), one may also set  
 728  $\Delta = 0$  and allow  $\{\mathbf{a}_i\}$  to fluctuate more freely, such that different boundary theories result.  
 729 In addition, we only consider the case that bulk is in the ground state. If the bulk contains  
 730 a topological defect, including both anyon excitations and  $\mathbf{G}$  symmetry defects, there must  
 731 be a corresponding anti-defect on the boundary. (Note that it is enough to consider only one  
 732 topological defect in the bulk. Multiple defects can always be fused into one.) This will make  
 733 at least one of the constraints  $\mathbf{A}_v = \mathbf{P}_l = \mathbf{1}$  to be violated at the boundary, corresponding to  
 734 insertion of twisted boundary conditions associated with the category symmetry  $\mathcal{C}_G$  in the 1D  
 735 systems.

## 736 5 Summary and outlook

737 In summary, we have constructed a 1D quantum lattice model that explicitly displays category  
 738 symmetry  $\mathcal{C}_G$ . The model can be viewed as an interpolation between the anyon chain model  
 739 and edge model of 2D bosonic SPTs, and as an edge model of 2D bosonic SETs. Our numerical  
 740 results show that the category symmetry constrains the model to the extent that it has a large  
 741 likelihood to be quantum critical. Hence, this model, with different input categories and tuning

742 parameters, is a good source for studying gapless phases. It is clear that more numerical effort  
743 is desired.

744 We discuss a few possible future directions.

- 745 1. One may generalize our model to  $\mathbf{G}$ -graded super or spin unitary fusion category (we  
746 notice that a related work is done in Ref. [56]). Super fusion category describes defects  
747 in fermionic systems, and spin fusion category is the corresponding category after gaug-  
748 ing fermion parity. [57,58] Our model can be readily generalized to spin fusion category,  
749 which has no difference to the usual unitary fusion category except that it has a special  
750 simple object, the fermion  $\psi$ . To make a connection to fermionic SPT/SET edges, one  
751 needs to find a way to ungauged the fermion parity, or equivalently gauge the dual sym-  
752 metry  $U(\psi)$ . This gauging procedure has been worked out in Ref. [37] in the example  
753 of Ising fusion category (the simplest spin fusion category). It is interesting to work out  
754 the general case and understand the connection to fermionic SPT/SET edges.
- 755 2. Another generalization is to make the variable  $x_i$  valued in a module category  $\mathcal{M}$  over  
756 a fusion category  $\mathcal{C}$  [16]. It is known that a general way to terminate the string-net  
757 model at the boundary is to use module category [59]. The recent study on duality of  
758 category symmetry in Ref. [33] precisely uses this language. The essence of having a  
759  $\mathbf{G}$ -grading structure in the input data  $\mathcal{C}_{\mathbf{G}}$  of our model is to enable a partial ungauging  
760 of the category symmetry. We expect that generalization to module category may help  
761 to ungauged general category symmetry in our model, which is essentially the duality  
762 discussed in Ref. [33].
- 763 3.  $\mathcal{C}_{\mathbf{G}}$  serves both as the input data and as the category that characterizes the symmetries of  
764 our model. However,  $\mathcal{C}_{\mathbf{G}}$  may not be the *maximal* category symmetry of the model. [60]  
765 For example, in the case that  $\mathcal{C}_{\mathbf{G}} = \mathcal{C}_{\text{Ising}}$  as input, the maximal category symmetry is  
766  $\mathcal{C}_{\text{Ising}} \times \overline{\mathcal{C}_{\text{Ising}}}$  when the low-energy physics is a critical Ising CFT. More generally, one  
767 may expect a larger category symmetry  $\mathcal{Z}(\mathcal{C}_{\mathbf{G}})$  (the Drinfeld center of  $\mathcal{C}_{\mathbf{G}}$ ) in the gapless  
768 state of the model [19]. Accordingly, in our construction, we have not made a full use  
769 of category symmetry in terms of constraining the low-energy physics. It is interesting  
770 to study how to construct the models with larger category symmetry.
- 771 4. It is also interesting to extend this construction to higher dimensions. In this perspective,  
772 one needs to make use of higher fusion categories [20–22].

## 773 Acknowledgements

774 We are grateful to Liang Kong, Tian Lan, Qing-Rui Wang, Wenjie Xi, Shizhong Zhang and Cuo-  
775 Yi Zhu for enlightening discussions. This work was supported by Research Grants Council of  
776 Hong Kong (GRF 11300819 and GRF 17311322) and National Natural Science Foundation of  
777 China (Grant No. 12222416). S.N. is also supported in part by Research Grants Council of  
778 Hong Kong under GRF 14302021 and NSFC/RGC Joint Research Scheme No. N-CUHK427/18,  
779 and by Direct Grant No. 4053416 from the Chinese University of Hong Kong.

## 780 A Symmetry and Hamiltonian

781 In this appendix, we give a derivation of the explicit expression (6) of the symmetry  $U(\mathbf{y}_h)$ .  
782 We also explicitly show that the Hamiltonian (8) is invariant under  $U(\mathbf{y}_h)$ .

783 **A.1 Derivation of Eq. (6)**

784 The graphical representation of  $U(y_h)$  is shown in Fig. 2. Under the action of  $U(y_h)$ , the  
 785 domain variables  $\alpha_i$  are simultaneously mapped to  $\mathbf{h}\alpha_i$ . Since  $\alpha_i^{-1}\alpha_{i+1}$  is unchanged, the do-  
 786 main wall defect  $\alpha_i$  keeps invariant under  $U(y_h)$ . Meanwhile, the variables  $x_i$  will be mapped  
 787 to other variables  $x'_i$

$$U(y_h) : |\{\alpha_i, x_i\}\rangle \rightarrow |\{\mathbf{h}\alpha_i, x'_i\}\rangle. \quad (69)$$

788 In general,  $U(y_h)|\{\alpha_i, x_i\}\rangle$  is a linear superposition of  $|\{\mathbf{h}\alpha_i, x'_i\}\rangle$ . Below we show that the  
 789 matrix element  $\langle\{\mathbf{h}\alpha_i, x'_i\}|U(y_h)|\{\alpha_i, x_i\}\rangle$  is given by (6). The derivation is divided into four  
 790 steps, as follows. Note that this derivation is equivalent to that for the usual anyon-chain  
 791 models [28].

792 1. Add a trivial line connecting  $y_h$  and  $x_{i+1}$  as in (70) and perform an  $F$  move which would

793 give an amplitude  $\left[ (F_{y_h}^{y_h x_{i+1} \overline{x_{i+1}}})^\dagger \right]_1^{x'_{i+1}} = \sqrt{\frac{d_{x'_{i+1}}}{d_{y_h} d_{x_{i+1}}}} \delta_{y_h x_{i+1} x'_{i+1}}$ . Here,  $\delta_{y_h x_{i+1} x'_{i+1}} = N_{y_h x_{i+1}}^{x'_{i+1}} = 0$   
 794 or 1. Summation over  $x'_{i+1}$  is not shown.

$$(70)$$

795 2. Perform a  $F$  move associated with the three defects  $y_h, x_i, a_{i+1}$ , with  $x'_{i+1}$  viewed as the  
 796 total fusion channel, as in (71). We call this procedure “sliding  $y_h$  across  $a_{i+1}$ ”. It gives

797 an amplitude  $\left[ (F_{x'_{i+1}}^{y_h, x_i, a_{i+1}})^\dagger \right]_{x_{i+1}}^{x'_i}$ .

$$(71)$$

798 3. Continue the second step, and keep sliding  $y_h$  across the rest  $a_j$ , as in (72). This gives

799 the amplitude  $\left[ \prod_{j \neq i, i+1} (F_{x'_{j+1}}^{y_h, x_j, a_{j+1}})^\dagger \right]_{x_{j+1}}^{x'_j} \left[ (F_{x''_{i+2}}^{y_h, x_{i+1}, a_{i+2}})^\dagger \right]_{x_{i+2}}^{x'_{i+1}}$ .

$$(72)$$

800 4. Shrink the “bubble” as in (73) which gives a coefficient  $\sqrt{\frac{d_{x_{i+1}} d_{y_h}}{d_{x'_{i+1}}}}$  and imposes the con-

801 dition  $x'_{i+1} = x''_{i+1}$ .

$$(73)$$

802 Combining all the steps and multiplying all the amplitudes, we obtain Eq. (6).

### 803 A.2 Hamiltonian is symmetric under $U(y_h)$

804 Now we show that the Hamiltonian (8) is symmetric under  $U(y_h)$  (6). Specifically, we show  
 805  $H_i U(y_h) = U(y_h) H_i$  when acting on any state. The graphical representation of  $U(y_h)$  in Fig. 2  
 806 has the advantage of being basis independent. We will make use of this and mainly work in  
 807 the basis (9). We will act  $H_i$  and  $U(y_h)$  on an arbitrary state in different orders, and compare  
 808 the final states, which turn to be the same.

809 On the one hand,

$$\begin{aligned}
 U(y_h) H_i \left| \begin{array}{c} a_{i-1} \quad a_i \quad a_{i+1} \\ \alpha_{i-1} \quad \alpha_i \quad \alpha_{i+1} \\ x_{i-1} \quad x_i \quad x_{i+1} \end{array} \right\rangle &= \sum_{z_i} [F_{x_{i+1}}^{x_{i-1} a_i a_{i+1}}]_{x_i}^{z_i} U(y_h) H_i \left| \begin{array}{c} a_i \quad a_{i+1} \\ \alpha_{i-1} \quad \alpha_{i+1} \\ x_{i-1} \quad x_{i+1} \end{array} \right\rangle \\
 &= \sum_{\alpha'_i} \sum_{z_i} w_{\alpha_i^{-1} \alpha'_i}^{z_i} [F_{x_{i+1}}^{x_{i-1} a_i a_{i+1}}]_{x_i}^{z_i} U(y_h) \left| \begin{array}{c} a'_i \quad a'_{i+1} \\ \alpha_{i-1} \quad \alpha_{i+1} \\ x_{i-1} \quad x_{i+1} \end{array} \right\rangle \\
 &= \sum_{\alpha'_i} \sum_{z_i} \sum_{\{x'_j | j \neq i\}} w_{\alpha_i^{-1} \alpha'_i}^{z_i} (F_{x_{i+1}}^{x_{i-1} a_i a_{i+1}})_{x_i}^{z_i} U_{\{x_i\}, y_h, z_i}^{\{x'_i\}} \left| \begin{array}{c} a'_i \quad h \alpha'_i \quad a'_{i+1} \\ h \alpha_{i-1} \quad z_i \quad h \alpha_{i+1} \\ x'_{i-1} \quad x'_{i+1} \end{array} \right\rangle
 \end{aligned}$$

$$(74)$$

810 where we have used the basis transformation (9) in the first line, and the definition (10) of  $H_i$

811 in the second line. The coefficient in the last line is

$$U_{\{x_i\}, y_h, z_i}^{\{x'_i\}} = \left( F_{x'_{i+1}}^{y_h, x_{i-1}, z_i} \right)_{x_{i+1}}^{\dagger x'_{i-1}} \prod_{j \neq i, i+1} \left( F_{x'_{j+1}}^{y_h, x_j, a_{j+1}} \right)_{x_{j+1}}^{\dagger x'_j}. \quad (75)$$



812 which is obtained in the same way as Appendix A.1. On the other hand,

$$\begin{aligned}
H_i U(y_h) \left| \begin{array}{c} \alpha_i \quad \alpha_{i+1} \\ \alpha_{i-1} \quad \alpha_i \quad \alpha_{i+1} \\ \hline x_{i-1} \quad x_i \quad x_{i+1} \end{array} \right\rangle &= \sum_{z_i} [F_{x_{i+1}}^{x_{i-1} \alpha_i \alpha_{i+1}}]_{x_i}^{z_i} H_i U(y_h) \left| \begin{array}{c} \alpha_i \quad \alpha_i \quad \alpha_{i+1} \\ \alpha_{i-1} \quad z_i \quad \alpha_{i+1} \\ \hline x_{i-1} \quad x_{i+1} \end{array} \right\rangle \\
&= \sum_{z_i} \sum_{\{x'_j | j \neq i\}} [F_{x_{i+1}}^{x_{i-1} \alpha_i \alpha_{i+1}}]_{x_i}^{z_i} U_{\{x_i, y_h, z_i\}}^{\{x'_i\}} H_i \left| \begin{array}{c} \alpha_i \quad \mathbf{h}\alpha_i \quad \alpha_{i+1} \\ \mathbf{h}\alpha_{i-1} \quad z_i \quad \mathbf{h}\alpha_{i+1} \\ \hline x'_{i-1} \quad x'_{i+1} \end{array} \right\rangle \\
&= \sum_{\alpha'_i} \sum_{z_i} \sum_{\{x'_j | j \neq i\}} (F_{x_{i+1}}^{x_{i-1} \alpha_i \alpha_{i+1}})^{z_i} U_{\{x_i, y_h, z_i\}}^{\{x'_i\}} w_{\alpha'_i}^{z_i} \left| \begin{array}{c} \mathbf{h}\alpha'_i \\ \mathbf{h}\alpha_{i-1} \quad z_i \quad \mathbf{h}\alpha_{i+1} \\ \hline x'_{i-1} \quad x'_{i+1} \end{array} \right\rangle
\end{aligned} \tag{76}$$

813 where we have used  $(\mathbf{h}\alpha_i)^{-1}(\mathbf{h}\alpha_{i+1}) = \alpha_i^{-1} \alpha_{i+1}$ . Comparing (74) and (76), we see the final  
814 expressions are exactly the same. As the initial state and  $i$  are arbitrary, we have proven  
815  $HU(y_h) = U(y_h)H$  for any  $y_h$ .

## 816 B Proof of $\text{Tr}(\mathbf{B}_p) = 1$ in $\mathcal{H}_{\{\alpha_i, \alpha_i, x_i\}}$

817 In this appendix, we show that  $\text{Tr}(\mathbf{B}_p) = 1$  in the space  $\mathcal{H}_{\{\alpha_i, \alpha_i, x_i\}}$  with given  $\{\alpha_i, \alpha_i, x_i\}$ . We  
818 will represent a state  $|\Psi\rangle$  in  $\mathcal{H}_{\{\alpha_i, \alpha_i, x_i\}}$  graphically as

$$|\Psi\rangle = \left| \begin{array}{c} y_L \\ \textcircled{\mathbf{g}_p} \alpha_L \end{array} \right\rangle \tag{77}$$

819 where  $y_L$  can be any simple object in  $\mathcal{C}_G$ ,  $\mathbf{g}_p = \alpha_L \mathbf{g}_{y_L}$ , and other spins on the lattice (Fig. 8(b))  
820 are omitted as  $\mathbf{B}_p$  does not act on them. Since  $\mathbf{g}_p$  is fixed by  $y_L$  and  $\alpha_L$ , the dimension of  
821  $\mathcal{H}_{\{\alpha_i, \alpha_i, x_i\}}$  is  $|\mathcal{C}_G|$ . The term  $\mathbf{B}_p$  is defined as  $\mathbf{B}_p = \frac{1}{D^2} \sum_{s \in \mathcal{C}_G} d_s \mathbf{B}_p^s \tilde{U}_p^{g_s}$ , where  $D = \sqrt{\sum_s d_s^2}$  and

$$\mathbf{B}_p^s \tilde{U}_p^{g_s} \left| \begin{array}{c} y_L \\ \textcircled{\mathbf{g}_p} \alpha_L \end{array} \right\rangle = \mathbf{B}_p^s \left| \begin{array}{c} y_L \\ \textcircled{\mathbf{g}_p \mathbf{g}_s} \alpha_L \end{array} \right\rangle = \left| \begin{array}{c} y_L \\ \textcircled{\textcircled{\mathbf{g}_p \mathbf{g}_s}} \alpha_L \end{array} \right\rangle = \sum_{y'_L} N_{y'_L}^{y_L} \left| \begin{array}{c} y'_L \\ \textcircled{\mathbf{g}_p \mathbf{g}_s} \alpha_L \end{array} \right\rangle \tag{78}$$

822 In the last equation, we have fused  $y_L$  and  $s$  strings, with  $N_{y'_L}^{y_L} = 0, 1$  being the fusion co-  
823 efficient. Note that individual action of  $\tilde{U}_p^{g_s}$  or  $\mathbf{B}_p^s$  goes out of the space  $\mathcal{H}_{\{\alpha_i, \alpha_i, x_i\}}$ . We have  
824 omitted arrows of the strings for simplicity, which can be easily restored.

825 We calculate  $\text{Tr}(\mathbf{B}_p)$  as follows:

$$\begin{aligned}
 \text{Tr}(\mathbf{B}_p) &= \sum_{y_L \in \mathcal{C}_G} \left\langle \alpha_L \left( \begin{array}{c} y_L \\ \mathfrak{g}_p \end{array} \right) \middle| \mathbf{B}_p \middle| \left( \begin{array}{c} y_L \\ \mathfrak{g}_p \end{array} \right) \alpha_L \right\rangle \\
 &= \sum_{y_L \in \mathcal{C}_G} \sum_{s \in \mathcal{C}_G} \frac{d_s}{D^2} \left\langle \alpha_L \left( \begin{array}{c} y_L \\ \mathfrak{g}_p \end{array} \right) \middle| \mathbf{B}_p^s \tilde{U}_p^{g_s} \middle| \left( \begin{array}{c} y_L \\ \mathfrak{g}_p \end{array} \right) \alpha_L \right\rangle \\
 &= \sum_{y_L \in \mathcal{C}_G} \sum_{s \in \mathcal{C}_G} \sum_{y'_L \in \mathcal{C}_G} \frac{d_s}{D^2} N_{y_L, s}^{y'_L} \left\langle \alpha_L \left( \begin{array}{c} y_L \\ \mathfrak{g}_p \end{array} \right) \middle| \left( \begin{array}{c} y'_L \\ \mathfrak{g}_p \mathfrak{g}_s \end{array} \right) \alpha_L \right\rangle \\
 &= \sum_{y_L \in \mathcal{C}_G} \sum_{s \in \mathcal{C}_G} \sum_{y'_L \in \mathcal{C}_G} \frac{d_s}{D^2} N_{y_L, s}^{y'_L} \delta_{y_L, y'_L} \delta_{\mathfrak{g}_s, 1} \\
 &= \sum_{y_L \in \mathcal{C}_G} \sum_{s \in \mathcal{C}_0} \frac{d_s}{D^2} N_{y_L, s}^{y_L} = \sum_{y_L \in \mathcal{C}_G} \frac{d_{y_L}^2}{D^2} = 1
 \end{aligned} \tag{79}$$

826 In the third line, we have inserted Eq. (78). In the last line, we have used  $\mathbf{d}_a = \mathbf{d}_{\bar{a}}$ ,  $N_{ab}^c = N_{a\bar{c}}^{\bar{b}}$   
 827 and  $\mathbf{d}_a \mathbf{d}_b = \sum_c \mathbf{d}_c N_{ab}^c$  for any  $\mathbf{a}, \mathbf{b}, \mathbf{c} \in \mathcal{C}_G$ , such that  $\sum_s \mathbf{d}_s N_{y_L, s}^{y_L} = \sum_s \mathbf{d}_s N_{y_L, \bar{y}_L}^{\bar{s}} = \mathbf{d}_{y_L}^2$ . Note  
 828 that if  $N_{y_L, s}^{y_L} \neq 0$ , we must have  $s \in \mathcal{C}_0$  due to the  $\mathbf{G}$ -grading structure in  $\mathcal{C}_G$ .

## 829 References

- 830 [1] Z.-C. Gu and X.-G. Wen, *Tensor-entanglement-filtering renormalization approach*  
 831 *and symmetry-protected topological order*, Phys. Rev. B **80**, 155131 (2009),  
 832 doi:[10.1103/PhysRevB.80.155131](https://doi.org/10.1103/PhysRevB.80.155131).
- 833 [2] X. Chen, Z.-C. Gu, Z.-X. Liu and X.-G. Wen, *Symmetry protected topological orders*  
 834 *and the group cohomology of their symmetry group*, Phys. Rev. B **87**, 155114 (2013),  
 835 doi:[10.1103/PhysRevB.87.155114](https://doi.org/10.1103/PhysRevB.87.155114).
- 836 [3] T. Senthil, *Symmetry-Protected Topological Phases of Quantum Matter*, Annual Review of  
 837 Condensed Matter Physics **6**, 299 (2015), doi:[10.1146/annurev-conmatphys-031214-](https://doi.org/10.1146/annurev-conmatphys-031214-014740)  
 838 [014740](https://doi.org/10.1146/annurev-conmatphys-031214-014740).
- 839 [4] M. Barkeshli, P. Bonderson, M. Cheng and Z. Wang, *Symmetry fractionalization,*  
 840 *defects, and gauging of topological phases*, Phys. Rev. B **100**, 115147 (2019),  
 841 doi:[10.1103/PhysRevB.100.115147](https://doi.org/10.1103/PhysRevB.100.115147).
- 842 [5] G. 't Hooft, *Naturalness, chiral symmetry, and spontaneous chiral symmetry breaking*,  
 843 NATO Sci. Ser. B **59**, 135 (1980), doi:[10.1007/978-1-4684-7571-5\\_9](https://doi.org/10.1007/978-1-4684-7571-5_9).
- 844 [6] E. Witten, *Fermion path integrals and topological phases*, Rev. Mod. Phys. **88**, 035001  
 845 (2016), doi:[10.1103/RevModPhys.88.035001](https://doi.org/10.1103/RevModPhys.88.035001).
- 846 [7] A. Vishwanath and T. Senthil, *Physics of three-dimensional bosonic topological insulators:*  
 847 *Surface-deconfined criticality and quantized magnetoelectric effect*, Phys. Rev. X **3**, 011016  
 848 (2013), doi:[10.1103/PhysRevX.3.011016](https://doi.org/10.1103/PhysRevX.3.011016).

- 849 [8] E. Lieb, T. Schultz and D. Mattis, *Two soluble models of an antiferromagnetic chain*, Annals  
850 of Physics **16**(3), 407 (1961), doi:[https://doi.org/10.1016/0003-4916\(61\)90115-4](https://doi.org/10.1016/0003-4916(61)90115-4).
- 851 [9] M. Oshikawa, *Commensurability, excitation gap, and topology in quantum many-*  
852 *particle systems on a periodic lattice*, Phys. Rev. Lett. **84**, 1535 (2000),  
853 doi:[10.1103/PhysRevLett.84.1535](https://doi.org/10.1103/PhysRevLett.84.1535).
- 854 [10] M. B. Hastings, *Lieb-schultz-mattis in higher dimensions*, Phys. Rev. B **69**, 104431 (2004),  
855 doi:[10.1103/PhysRevB.69.104431](https://doi.org/10.1103/PhysRevB.69.104431).
- 856 [11] M. Cheng, M. Zaletel, M. Barkeshli, A. Vishwanath and P. Bonderson, *Translational sym-*  
857 *metry and microscopic constraints on symmetry-enriched topological phases: A view from*  
858 *the surface*, Phys. Rev. X **6**, 041068 (2016), doi:[10.1103/PhysRevX.6.041068](https://doi.org/10.1103/PhysRevX.6.041068).
- 859 [12] D. Gaiotto, A. Kapustin, N. Seiberg and B. Willett, *Generalized global symmetries*, Journal  
860 of High Energy Physics **2015**, 172 (2015), doi:[10.1007/JHEP02\(2015\)172](https://doi.org/10.1007/JHEP02(2015)172), [1412.5148](https://arxiv.org/abs/1412.5148).
- 861 [13] A. Kapustin and N. Seiberg, *Coupling a QFT to a TQFT and duality*, Journal of High  
862 Energy Physics **2014**, 1 (2014), doi:[10.1007/JHEP04\(2014\)001](https://doi.org/10.1007/JHEP04(2014)001), [1401.0740](https://arxiv.org/abs/1401.0740).
- 863 [14] A. Y. Kitaev, *Fault-tolerant quantum computation by anyons*, Annals of Physics **303**(1), 2  
864 (2003), doi:[10.1016/S0003-4916\(02\)00018-0](https://doi.org/10.1016/S0003-4916(02)00018-0), [quant-ph/9707021](https://arxiv.org/abs/quant-ph/9707021).
- 865 [15] G. W. Moore and N. Seiberg, *Classical and Quantum Conformal Field Theory*, Commun.  
866 Math. Phys. **123**, 177 (1989), doi:[10.1007/BF01238857](https://doi.org/10.1007/BF01238857).
- 867 [16] V. Ostrik, D. Nikshych, P. Etingof and S. Gelaki, *Tensor Categories*, American Mathematical  
868 Society, Providence, Rhode Island (2015).
- 869 [17] C.-M. Chang, Y.-H. Lin, S.-H. Shao, Y. Wang and X. Yin, *Topological defect lines and*  
870 *renormalization group flows in two dimensions*, Journal of High Energy Physics **2019**(1),  
871 26 (2019), doi:[10.1007/JHEP01\(2019\)026](https://doi.org/10.1007/JHEP01(2019)026), [1802.04445](https://arxiv.org/abs/1802.04445).
- 872 [18] L. Bhardwaj and Y. Tachikawa, *On finite symmetries and their gauging in two dimensions*,  
873 Journal of High Energy Physics **2018**(3), 189 (2018), doi:[10.1007/JHEP03\(2018\)189](https://doi.org/10.1007/JHEP03(2018)189),  
874 [1704.02330](https://arxiv.org/abs/1704.02330).
- 875 [19] W. Ji and X.-G. Wen, *Categorical symmetry and noninvertible anomaly in symmetry-*  
876 *breaking and topological phase transitions*, Phys. Rev. Res. **2**, 033417 (2020),  
877 doi:[10.1103/PhysRevResearch.2.033417](https://doi.org/10.1103/PhysRevResearch.2.033417).
- 878 [20] C. L. Douglas and D. J. Reutter, *Fusion 2-categories and a state-sum invariant for 4-*  
879 *manifolds*, arXiv e-prints arXiv:1812.11933 (2018), [1812.11933](https://arxiv.org/abs/1812.11933).
- 880 [21] D. Gaiotto and T. Johnson-Freyd, *Symmetry protected topological phases and*  
881 *generalized cohomology*, Journal of High Energy Physics **2019**(5), 7 (2019),  
882 doi:[10.1007/JHEP05\(2019\)007](https://doi.org/10.1007/JHEP05(2019)007), [1712.07950](https://arxiv.org/abs/1712.07950).
- 883 [22] L. Kong, T. Lan, X.-G. Wen, Z.-H. Zhang and H. Zheng, *Algebraic higher symmetry and*  
884 *categorical symmetry: A holographic and entanglement view of symmetry*, Phys. Rev. Res.  
885 **2**, 043086 (2020), doi:[10.1103/PhysRevResearch.2.043086](https://doi.org/10.1103/PhysRevResearch.2.043086).
- 886 [23] L. Kong and H. Zheng, *Categories of quantum liquids I*, arXiv e-prints arXiv:2011.02859  
887 (2020), [2011.02859](https://arxiv.org/abs/2011.02859).
- 888 [24] L. Kong and H. Zheng, *Categories of quantum liquids II*, arXiv e-prints arXiv:2107.03858  
889 (2021), [2107.03858](https://arxiv.org/abs/2107.03858).

- 890 [25] L. Kong and H. Zheng, *Categories of quantum liquids I*, Journal of High Energy Physics  
891 **2022**(8), 70 (2022), doi:[10.1007/JHEP08\(2022\)070](https://doi.org/10.1007/JHEP08(2022)070), [2201.05726](https://arxiv.org/abs/2201.05726).
- 892 [26] D. S. Freed, G. W. Moore and C. Teleman, *Topological symmetry in quantum field theory*,  
893 arXiv e-prints arXiv:2209.07471 (2022), [2209.07471](https://arxiv.org/abs/2209.07471).
- 894 [27] R. Thorngren and Y. Wang, *Fusion Category Symmetry I: Anomaly In-Flow and Gapped*  
895 *Phases*, arXiv e-prints arXiv:1912.02817 (2019), [1912.02817](https://arxiv.org/abs/1912.02817).
- 896 [28] A. Feiguin, S. Trebst, A. W. W. Ludwig, M. Troyer, A. Kitaev, Z. Wang and M. H. Freedman,  
897 *Interacting anyons in topological quantum liquids: The golden chain*, Phys. Rev. Lett. **98**,  
898 160409 (2007), doi:[10.1103/PhysRevLett.98.160409](https://doi.org/10.1103/PhysRevLett.98.160409).
- 899 [29] C. Gils, E. Ardonne, S. Trebst, D. A. Huse, A. W. W. Ludwig, M. Troyer and Z. Wang,  
900 *Anyonic quantum spin chains: Spin-1 generalizations and topological stability*, Phys. Rev.  
901 B **87**, 235120 (2013), doi:[10.1103/PhysRevB.87.235120](https://doi.org/10.1103/PhysRevB.87.235120).
- 902 [30] R. N. C. Pfeifer, O. Buerschaper, S. Trebst, A. W. W. Ludwig, M. Troyer and G. Vidal, *Trans-*  
903 *lation invariance, topology, and protection of criticality in chains of interacting anyons*,  
904 Phys. Rev. B **86**, 155111 (2012), doi:[10.1103/PhysRevB.86.155111](https://doi.org/10.1103/PhysRevB.86.155111).
- 905 [31] D. Aasen, R. S. K. Mong and P. Fendley, *Topological defects on the lattice: I. the ising*  
906 *model*, Journal of Physics A: Mathematical and Theoretical **49**(35), 354001 (2016),  
907 doi:[10.1088/1751-8113/49/35/354001](https://doi.org/10.1088/1751-8113/49/35/354001).
- 908 [32] D. Aasen, P. Fendley and R. S. K. Mong, *Topological Defects on the Lattice: Dualities and*  
909 *Degeneracies*, arXiv e-prints arXiv:2008.08598 (2020), [2008.08598](https://arxiv.org/abs/2008.08598).
- 910 [33] L. Lootens, C. Delcamp, G. Ortiz and F. Verstraete, *Dualities in one-dimensional quantum*  
911 *lattice models: symmetric Hamiltonians and matrix product operator intertwiners*, arXiv  
912 e-prints arXiv:2112.09091 (2021), [2112.09091](https://arxiv.org/abs/2112.09091).
- 913 [34] X. Chen, Z.-X. Liu and X.-G. Wen, *Two-dimensional symmetry-protected topological or-*  
914 *ders and their protected gapless edge excitations*, Phys. Rev. B **84**, 235141 (2011),  
915 doi:[10.1103/PhysRevB.84.235141](https://doi.org/10.1103/PhysRevB.84.235141).
- 916 [35] M. Levin and Z.-C. Gu, *Braiding statistics approach to symmetry-protected topological*  
917 *phases*, Phys. Rev. B **86**, 115109 (2012), doi:[10.1103/PhysRevB.86.115109](https://doi.org/10.1103/PhysRevB.86.115109).
- 918 [36] C. Bao, S. Yang, C. Wang and Z.-C. Gu, *Lattice model constructions for gapless*  
919 *domain walls between topological phases*, Phys. Rev. Research **4**, 023038 (2022),  
920 doi:[10.1103/PhysRevResearch.4.023038](https://doi.org/10.1103/PhysRevResearch.4.023038).
- 921 [37] R. A. Jones and M. A. Metlitski, *One-dimensional lattice models for the boundary*  
922 *of two-dimensional majorana fermion symmetry-protected topological phases: Kramers-*  
923 *wannier duality as an exact  $Z_2$  symmetry*, Phys. Rev. B **104**, 245130 (2021),  
924 doi:[10.1103/PhysRevB.104.245130](https://doi.org/10.1103/PhysRevB.104.245130).
- 925 [38] C. Heinrich, F. Burnell, L. Fidkowski and M. Levin, *Symmetry-enriched string*  
926 *nets: Exactly solvable models for set phases*, Phys. Rev. B **94**, 235136 (2016),  
927 doi:[10.1103/PhysRevB.94.235136](https://doi.org/10.1103/PhysRevB.94.235136).
- 928 [39] M. Cheng, Z.-C. Gu, S. Jiang and Y. Qi, *Exactly solvable models for symmetry-enriched*  
929 *topological phases*, Phys. Rev. B **96**, 115107 (2017), doi:[10.1103/PhysRevB.96.115107](https://doi.org/10.1103/PhysRevB.96.115107).

- 930 [40] A. Kitaev, *Anyons in an exactly solved model and beyond*, Annals of Physics **321**(1), 2  
931 (2006), doi:<http://dx.doi.org/10.1016/j.aop.2005.10.005>.
- 932 [41] P. Etingof, D. Nikshych and V. Ostrik, *Fusion categories and homotopy theory*, Quantum  
933 Topol **1**, 209 (2010), doi:[10.4171/QT/6](https://doi.org/10.4171/QT/6).
- 934 [42] M. Buican and A. Gromov, *Anyonic Chains, Topological Defects, and Conformal*  
935 *Field Theory*, Communications in Mathematical Physics **356**(3), 1017 (2017),  
936 doi:[10.1007/s00220-017-2995-6](https://doi.org/10.1007/s00220-017-2995-6), [1701.02800](https://arxiv.org/abs/1701.02800).
- 937 [43] K. Kawagoe and M. Levin, *Anomalies in bosonic symmetry-protected topological edge the-*  
938 *ories: Connection to  $f$  symbols and a method of calculation*, Phys. Rev. B **104**, 115156  
939 (2021), doi:[10.1103/PhysRevB.104.115156](https://doi.org/10.1103/PhysRevB.104.115156).
- 940 [44] T. Giamarchi, *Quantum Physics in One Dimension*, Oxford University Press (2003).
- 941 [45] D. Tambara and S. Yamagami, *Tensor categories with fusion rules of self-*  
942 *duality for finite abelian groups*, Journal of Algebra **209**(2), 692 (1998),  
943 doi:<https://doi.org/10.1006/jabr.1998.7558>.
- 944 [46] S. R. White, *Density matrix formulation for quantum renormalization groups*, Phys. Rev.  
945 Lett. **69**, 2863 (1992), doi:[10.1103/PhysRevLett.69.2863](https://doi.org/10.1103/PhysRevLett.69.2863).
- 946 [47] P. Francesco, P. Mathieu and D. Sénéchal, *Conformal Field Theory*, Springer-Verlag New  
947 York, Inc. (1997).
- 948 [48] P. Calabrese and J. Cardy, *Entanglement entropy and quantum field theory*, Journal of Sta-  
949 *tistical Mechanics: Theory and Experiment* **2004**(6), 06002 (2004), doi:[10.1088/1742-](https://doi.org/10.1088/1742-5468/2004/06/P06002)  
950 [5468/2004/06/P06002](https://doi.org/10.1088/1742-5468/2004/06/P06002), [hep-th/0405152](https://arxiv.org/abs/hep-th/0405152).
- 951 [49] M. Fishman, S. R. White and E. M. Stoudenmire, *The ITensor Software Li-*  
952 *brary for Tensor Network Calculations*, SciPost Phys. Codebases p. 4 (2022),  
953 doi:[10.21468/SciPostPhysCodeb.4](https://doi.org/10.21468/SciPostPhysCodeb.4).
- 954 [50] P. Ginsparg, *Curiosities at  $c = 1$* , Nuclear Physics B **295**(2), 153 (1988),  
955 doi:[https://doi.org/10.1016/0550-3213\(88\)90249-0](https://doi.org/10.1016/0550-3213(88)90249-0).
- 956 [51] A. Kirillov and N. Reshetikhin, *Representations of the algebra  $U_q(\mathfrak{sl}(2))$ ,  $q$ -orthogonal*  
957 *polynomials and invariants of links*, in V.G. Kac, ed, Infinite dimensional Lie algebras and  
958 groups, Proceedings of the conference held at CIRM, Luminy, Marseille, p. 285, World  
959 Scientific, Singapore (1988).
- 960 [52] Q.-R. Wang, S.-Q. Ning and M. Cheng, *Domain Wall Decorations, Anomalies and Spectral*  
961 *Sequences in Bosonic Topological Phases*, arXiv e-prints arXiv:2104.13233 (2021), [2104.](https://arxiv.org/abs/2104.13233)  
962 [13233](https://arxiv.org/abs/2104.13233).
- 963 [53] T. Scaffidi, D. E. Parker and R. Vasseur, *Gapless symmetry-protected topological order*,  
964 Phys. Rev. X **7**, 041048 (2017), doi:[10.1103/PhysRevX.7.041048](https://doi.org/10.1103/PhysRevX.7.041048).
- 965 [54] R. Thorngren, A. Vishwanath and R. Verresen, *Intrinsically gapless topological phases*,  
966 Phys. Rev. B **104**, 075132 (2021), doi:[10.1103/PhysRevB.104.075132](https://doi.org/10.1103/PhysRevB.104.075132).
- 967 [55] Y. Hu, S. D. Stirling and Y.-S. Wu, *Ground-state degeneracy in the levin-wen model for*  
968 *topological phases*, Phys. Rev. B **85**, 075107 (2012), doi:[10.1103/PhysRevB.85.075107](https://doi.org/10.1103/PhysRevB.85.075107).
- 969 [56] Q.-R. Wang and et al., , unpublished .

- 970 [57] P. Bruillard, C. Galindo, T. Hagge, S.-H. Ng, J. Y. Plavnik, E. C. Rowell and Z. Wang,  
971 *Fermionic modular categories and the 16-fold way*, Journal of Mathematical Physics **58**(4),  
972 041704 (2017), doi:[10.1063/1.4982048](https://doi.org/10.1063/1.4982048), [1603.09294](https://arxiv.org/abs/1603.09294).
- 973 [58] T. Johnson-Freyd and D. Reutter, *Minimal nondegenerate extensions*, arXiv e-prints  
974 arXiv:2105.15167 (2021), [2105.15167](https://arxiv.org/abs/2105.15167).
- 975 [59] A. Kitaev and L. Kong, *Models for Gapped Boundaries and Domain Walls*, Communications  
976 in Mathematical Physics **313**(2), 351 (2012), doi:[10.1007/s00220-012-1500-5](https://doi.org/10.1007/s00220-012-1500-5), [1104.](https://arxiv.org/abs/1104.5047)  
977 [5047](https://arxiv.org/abs/1104.5047).
- 978 [60] A. Chatterjee, W. Ji and X.-G. Wen, *Emergent maximal categorical symmetry in a gapless*  
979 *state*, arXiv e-prints arXiv:2212.14432 (2022), [2212.14432](https://arxiv.org/abs/2212.14432).